The Superconducting Quantum Interference Device: Principles and Applications

- A SQUID primer
- The diversity of SQUIDs
- Searching for axions: the microstrip SQUID amplifier
- Microtesla NMR and MRI

Supported by DOE

LBNL
18 May 2005

Superconductivity

A macroscopic quantum state

Condensate of Cooper pairs

Charge 2e, **k** = 0, s= 0

Low-T_c : Electron-phonon interaction

High-T_c : ???

$$\Psi(\vec{r},t) = |\Psi(\vec{r},t)|\, e^{i\phi(\vec{r},t)}$$

Flux quantization

Single-valuedness of Ψ:

$\Phi = n\Phi_0$ ($n = 0, \pm1, \pm2, \ldots$)

where

$\Phi_0 \equiv h/2e \approx 2 \times 10^{-15}$ Wb

is the flux quantum

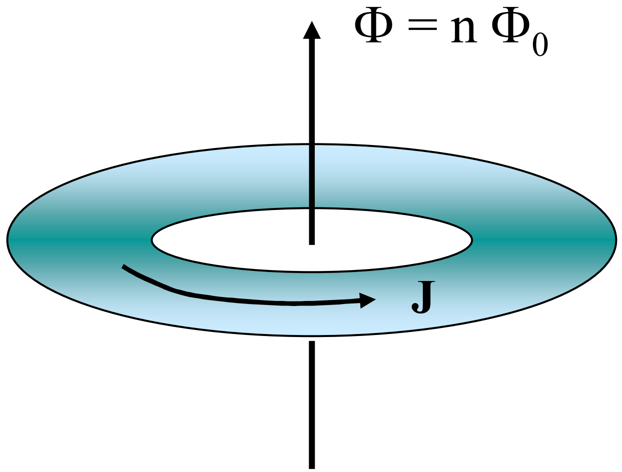

Josephson Tunneling

- Cooper pairs tunnel through barrier

Brian Josephson 1962

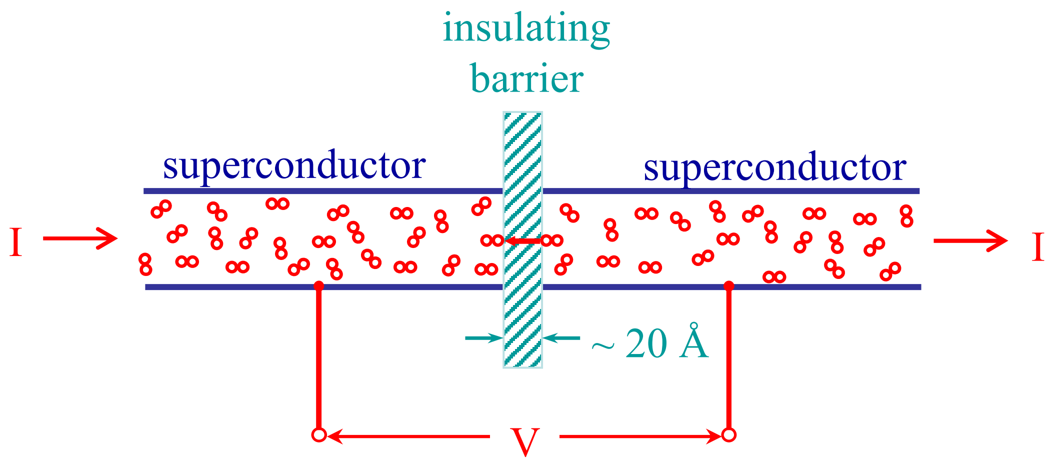

$$I = I_0 \sin\delta$$
where I_0 = critical current
$$\delta = \phi_1 - \phi_2$$
$$d\delta/dt = 2eV/\hbar$$
$$= 2\pi V/\Phi_0$$

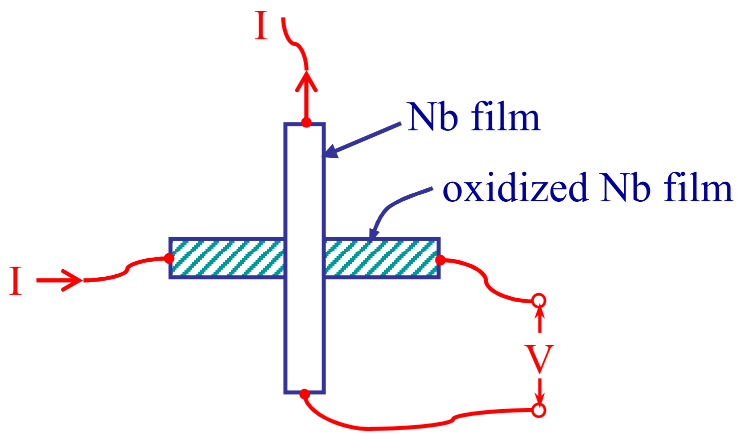

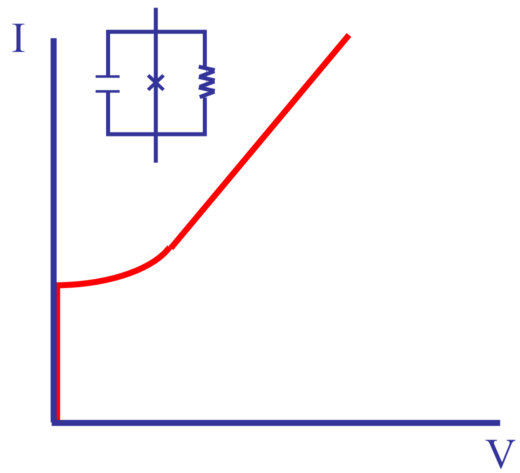

The dc Superconducting Quantum Interference Device

- **dc SQUID**

  Two Josephson junctions on a superconducting ring

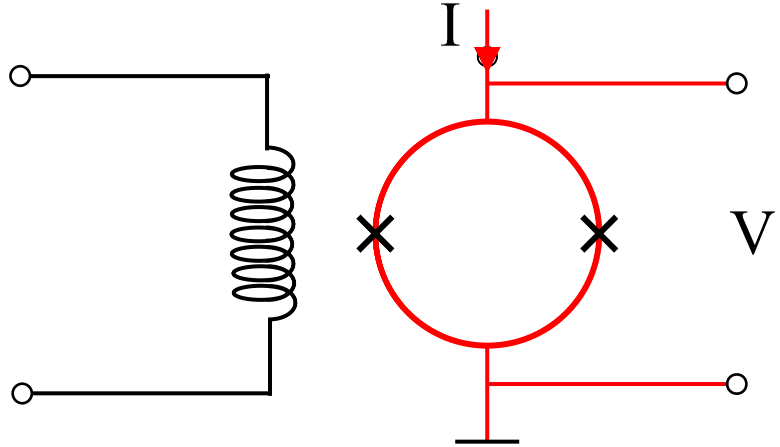

- **Current-voltage (I-V) characteristic modulated by magnetic flux Φ:**

  Period one flux quantum $\Phi_o = h/2e = 2 \times 10^{-15}$ T m^2

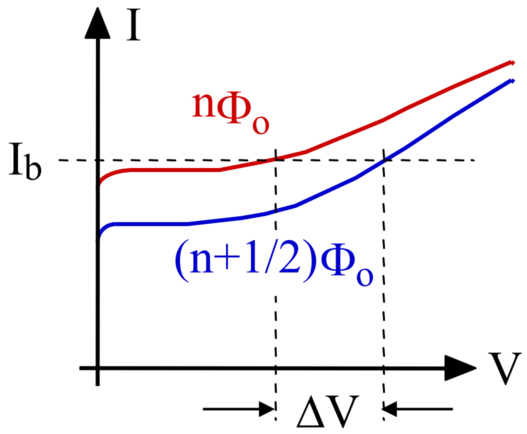

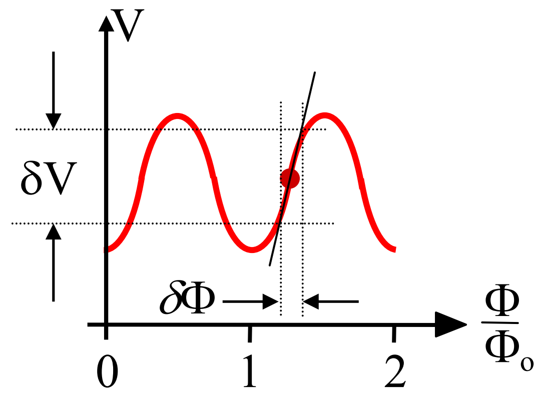

Low-T_c SQUID

Operating temperature: 4.2 K

Multilayer device: niobium - aluminum oxide - niobium

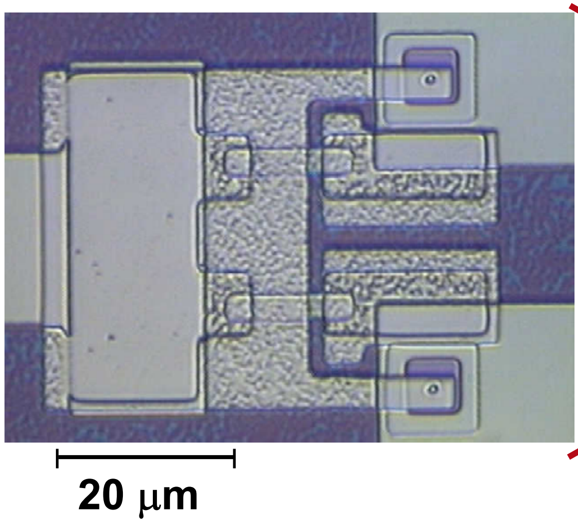

Josephson junctions

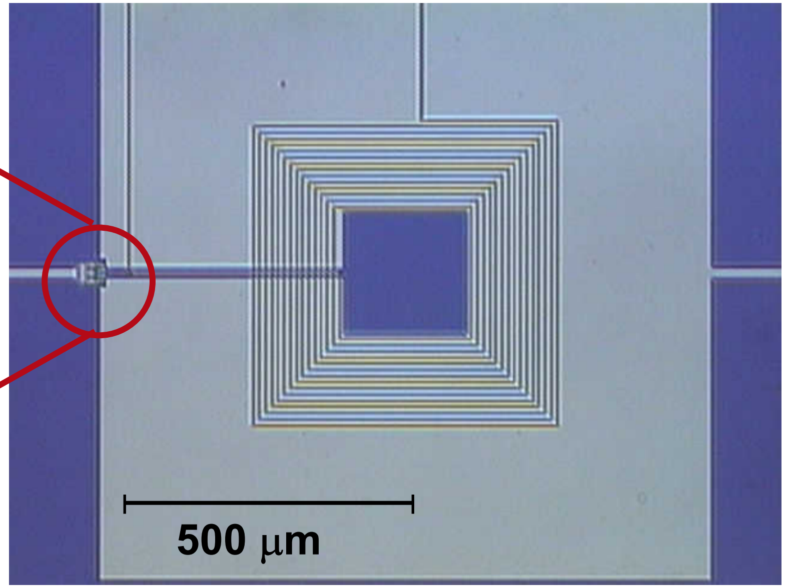

Nb-AlOx-Nb SQUID
with input coil

The Flux-Locked Loop

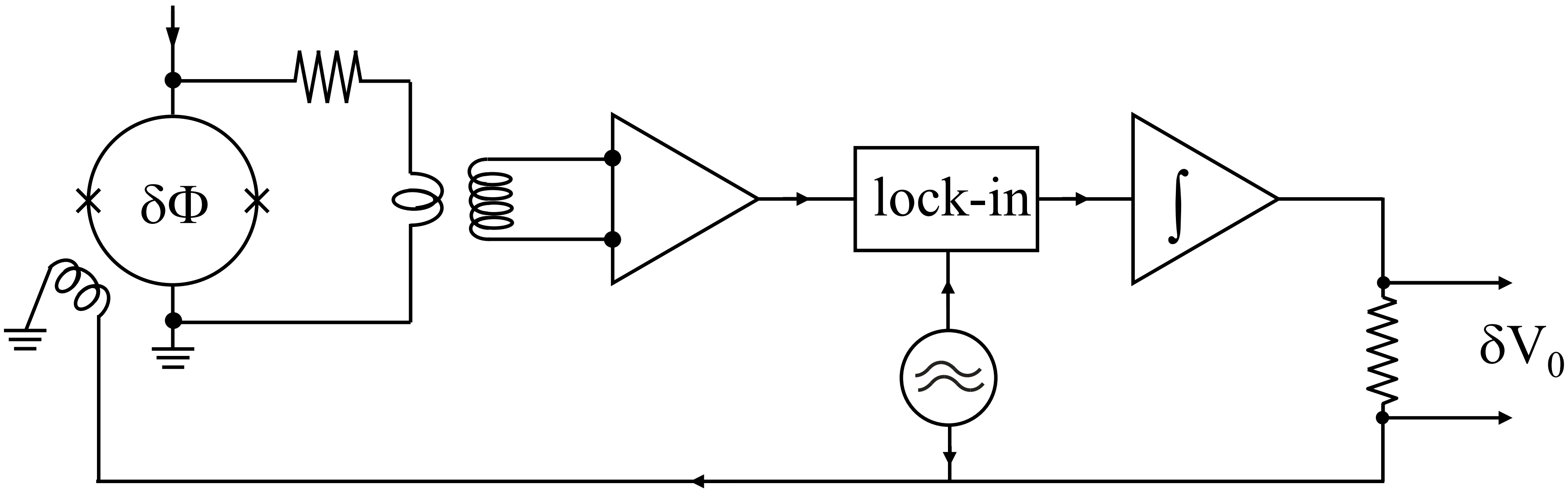

- Linear response: $\delta V_0 \propto \delta\Phi$
- Large dynamic range: $\delta\Phi >> \Phi_0$
- Can detect minute flux changes: $\delta\Phi << \Phi_0$

Spectral Density of Flux Noise in a dc SQUID

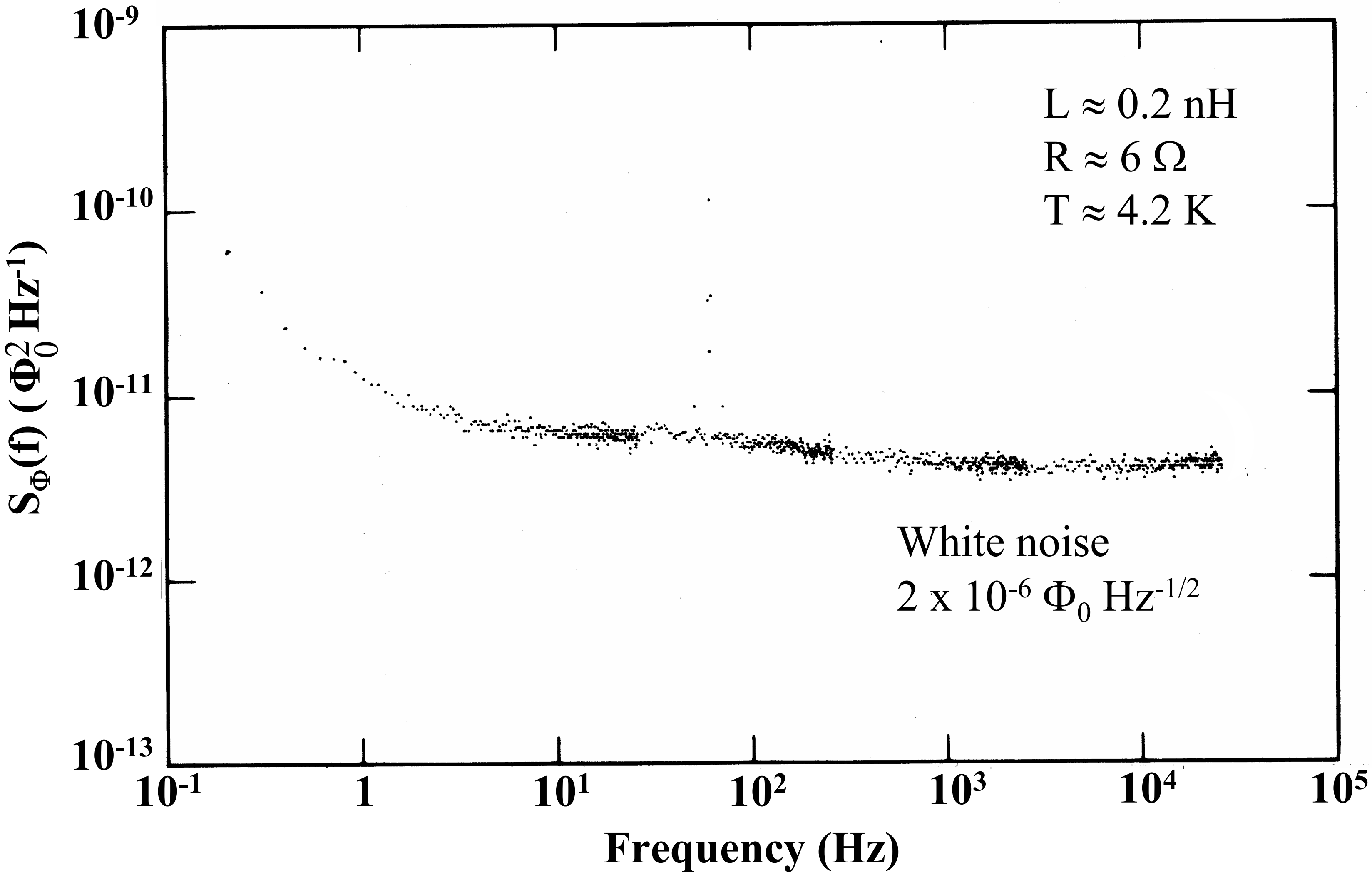

Fred Wellstood 1984

Approximate Theory for Flux Noise in the DC SQUID

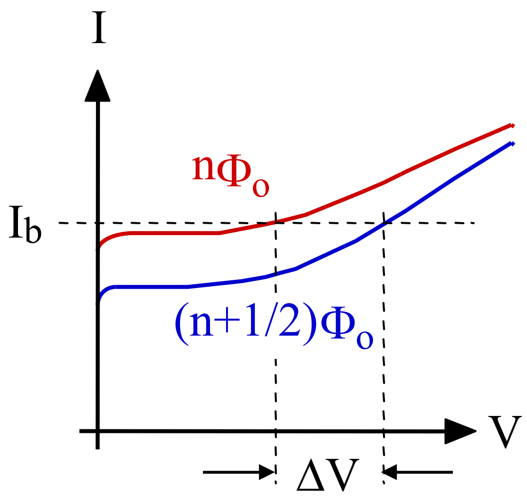

L is the SQUID inductance

R is the shunt resistance for each junction

Maximum change in critical current $\Delta I_c \sim \Phi_0/L$

Corresponding change in voltage $\Delta V \sim \Phi_0 R/L$

Flux-to-voltage transfer function $(\partial V/ \partial \Phi)_I \sim R/L$

Spectral density of voltage noise $S_v(f) \sim 4\, k_B T R$

Spectral density of flux noise $S_\Phi(f) \sim 4\, k_B T R/(\partial V/ \partial \Phi)_I^2$

$\sim 4\, k_B T L^2/R$

Computed Theory for Flux Noise in the DC SQUID

The SQUID is optimized for $\beta_L \equiv 2LI_0/\Phi_0 = 1$, $\beta_c \equiv 2\pi I_0 CR^2/\Phi_0 = 1$

Computed $S_\Phi(f) \approx 16\ k_B T L^2/R$

Noise energy $\varepsilon(f) \equiv S_\Phi(f)/2L \approx 9 k_B T/(R/L)$

Comparison with Experiment

For $L = 200$ pH, $R = 6\ \Omega$, $T = 4.2$ K:

$S_\Phi(f) \approx 1.2 \times 10^{-6}\ \Phi_0\ \mathrm{Hz}^{-1/2}$

$\varepsilon(f) \approx 1.5 \times 10^{-32}\ \mathrm{JHz}^{-1} \approx 150\hbar$

How Big is 10^{-32} J ($\sim 10^{-13}$ eV)?

This is the energy required to raise 1 electron

through 1 mm in the earth's gravitational field

$$mgx \approx 10^{-30}\ \text{kg}.10\ \text{ms}^{-2}.10^{-3}\ \text{m} \approx 10^{-32}\ \text{J}$$

OR

10^{-14} x the ground state energy of one hydrogen atom

Superconducting Flux Transformer: Magnetometer and Gradiometer

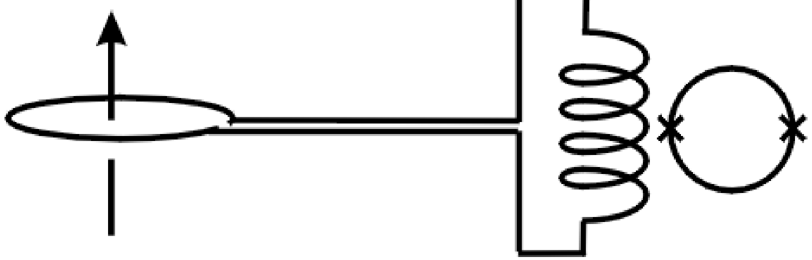

$B_N \sim 1$ fT Hz$^{-1/2}$

Flux-locked SQUID

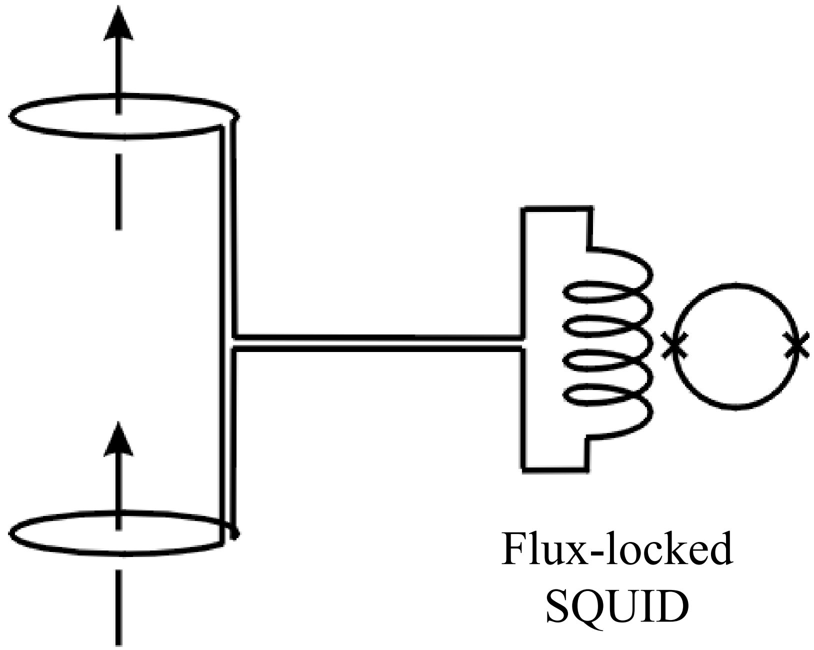

Flux-locked SQUID

Magnetic Fields

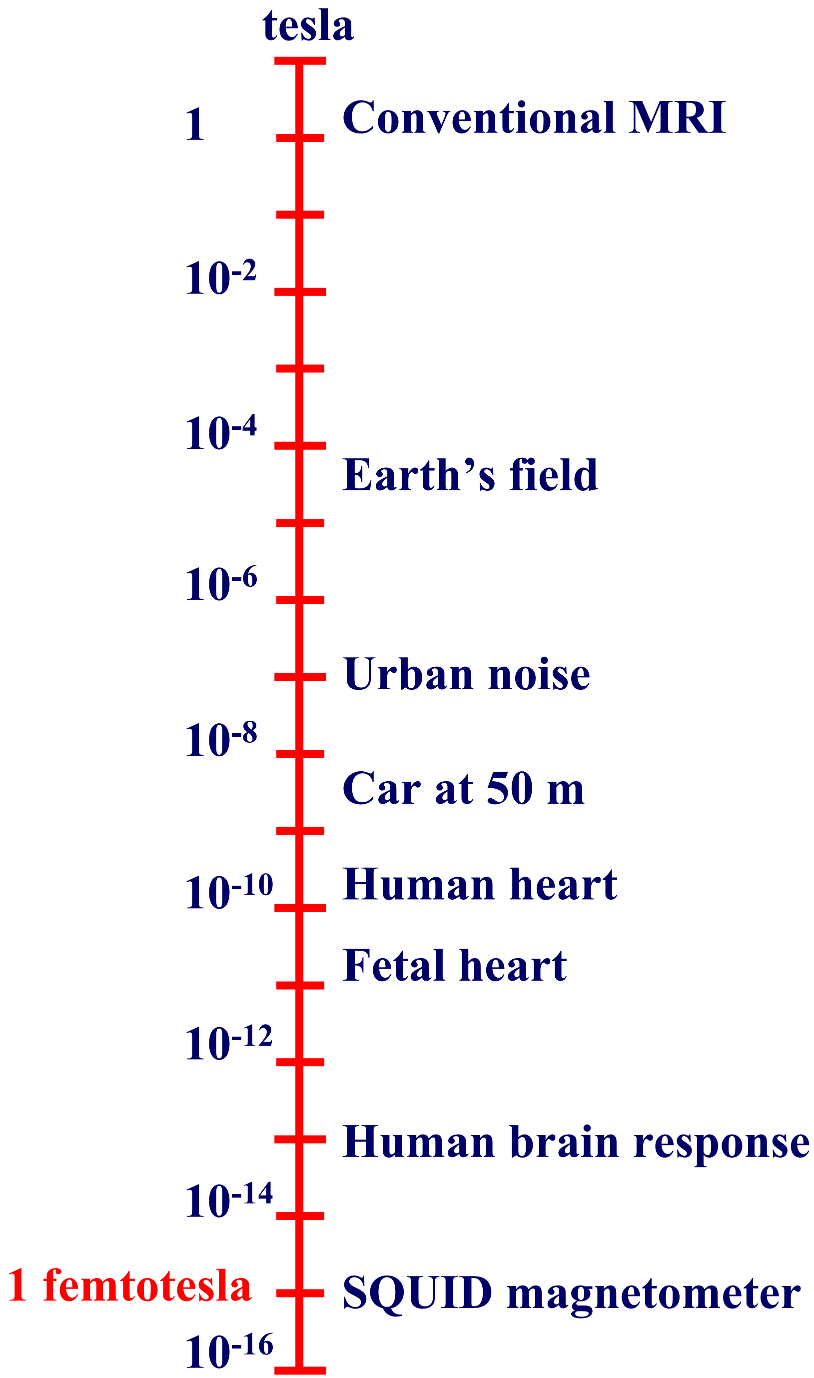

SQUID Femtovoltmeter

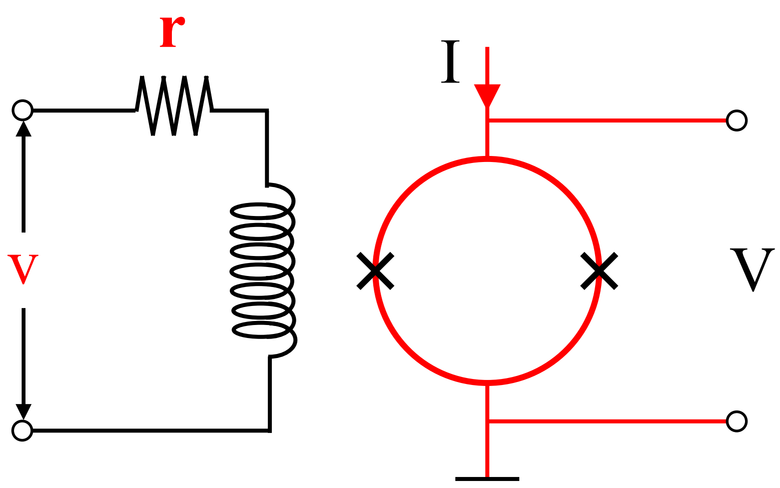

For $r = 10^{-8}\ \Omega$, $T = 4.2$ K

Johnson noise $\approx 10^{-15}$ V Hz$^{-1/2}$

The Diversity of SQUIDs

Quantum Design "Evercool"

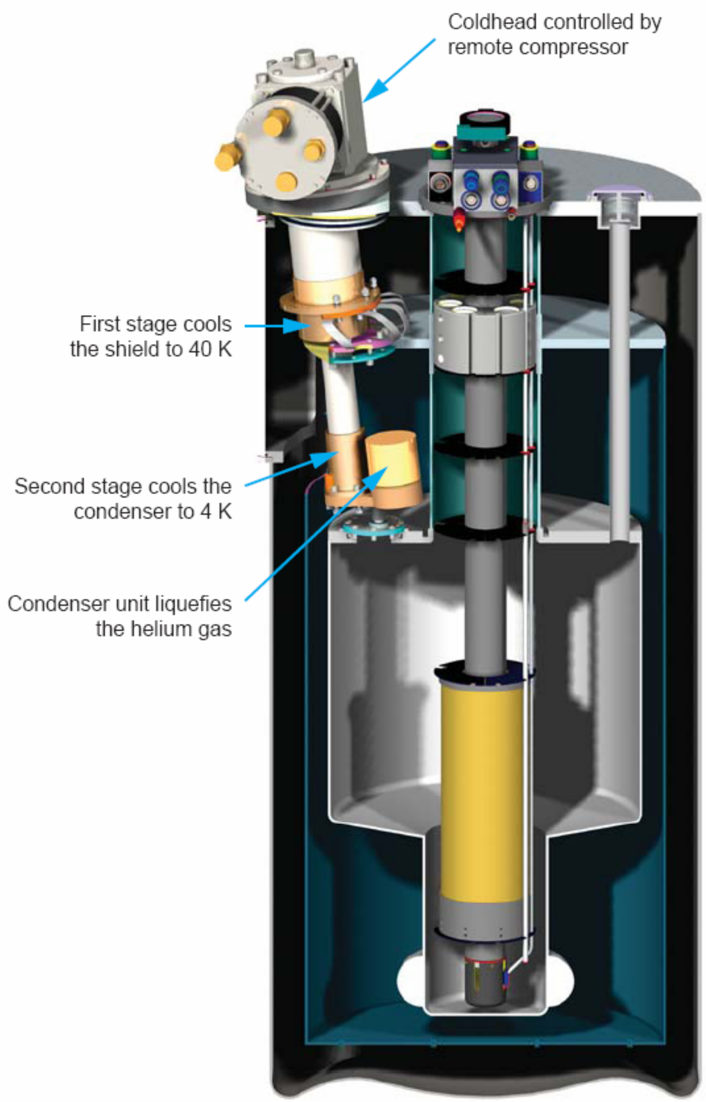

Cut-away Dewar View

2G Superconducting Rock Magnetometer

SQUID Surveying for Minerals

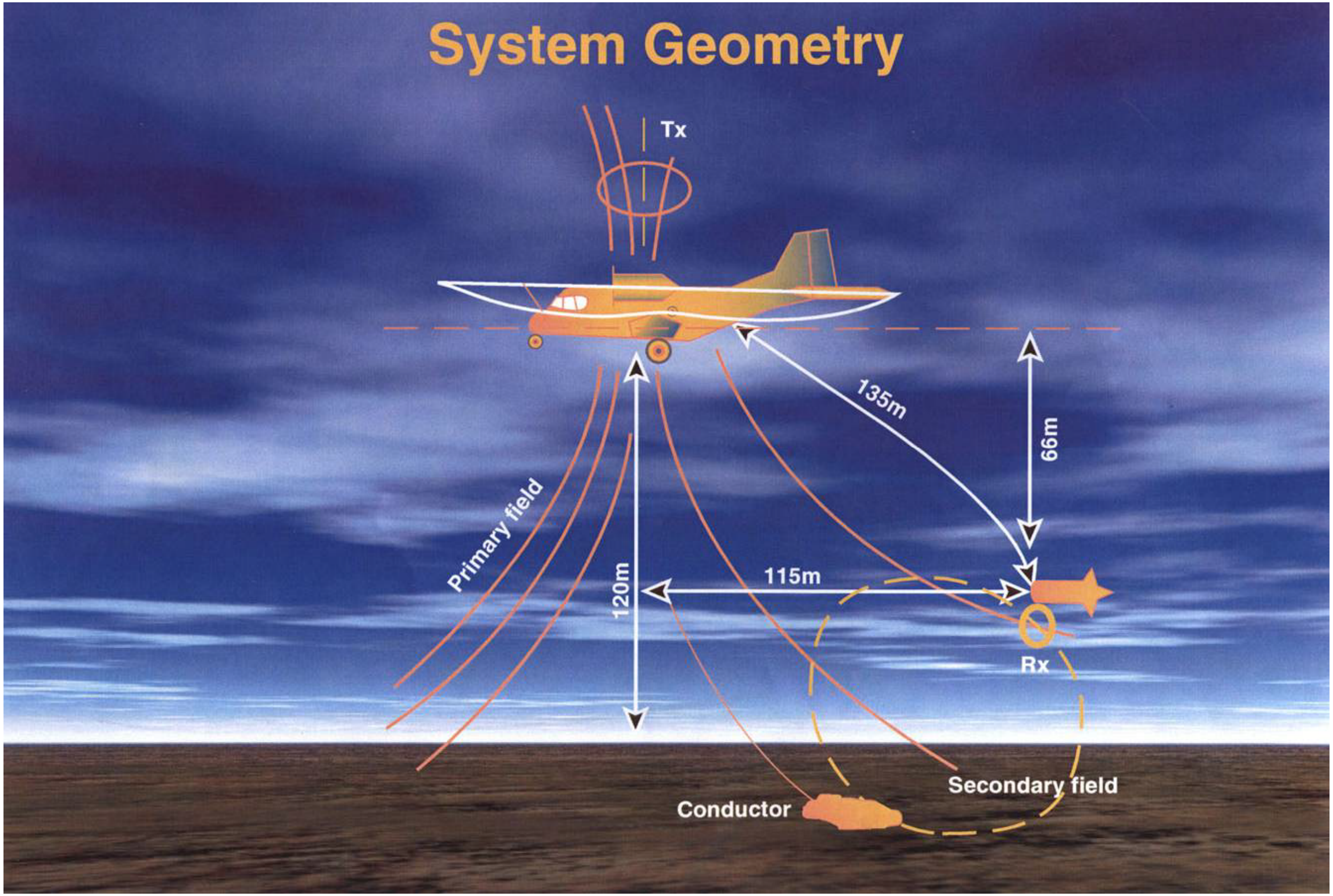

Courtesy Cathey Foley (CSIRO)

MAGMA-C1 Scanning SQUID Microscope
Neocera, Inc.

A Non-Contact, Non-Destructive Next Generation Imaging tool for the Semiconductor Industry's complex devices, advanced packages, and full assemblies

Atacama Pathfinder EXperiment

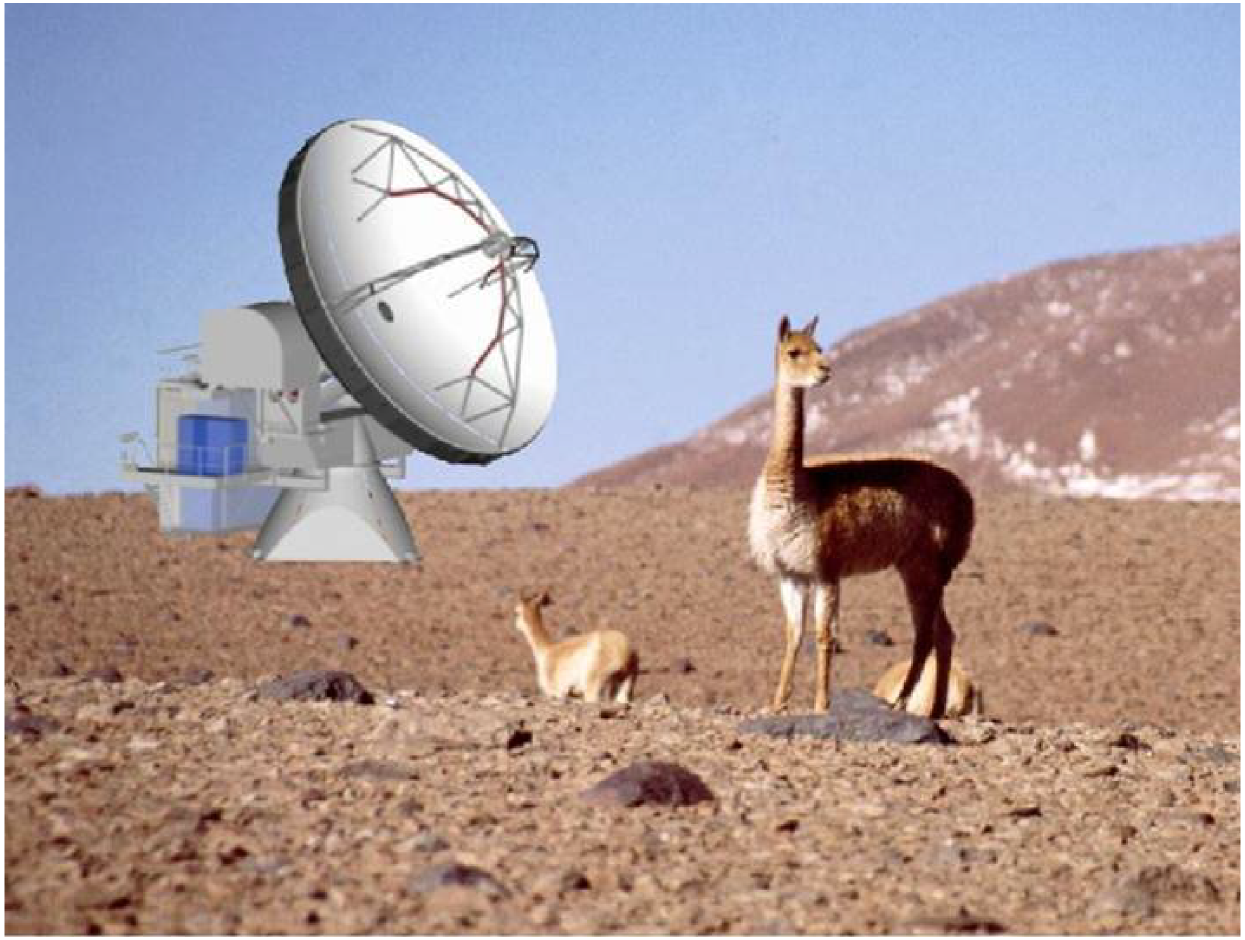

Gravity Probe-B

Tests of General Relativity

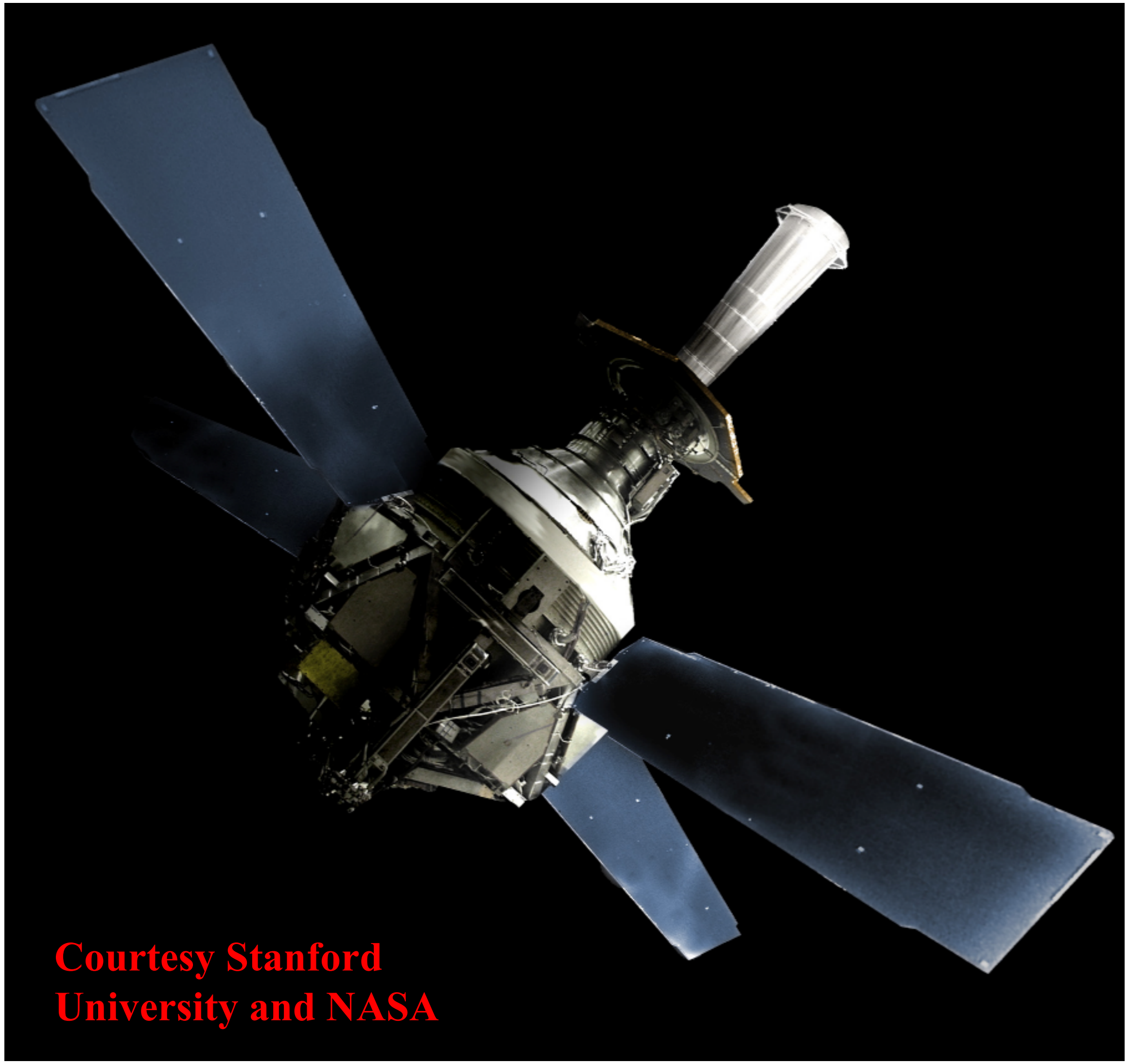

- Geodetic effect—curved space-time due to the presence of the Earth
- Lense-Thirring effect—dragging of the local space-time frame due to rotation

UC Berkeley Flux Qubits

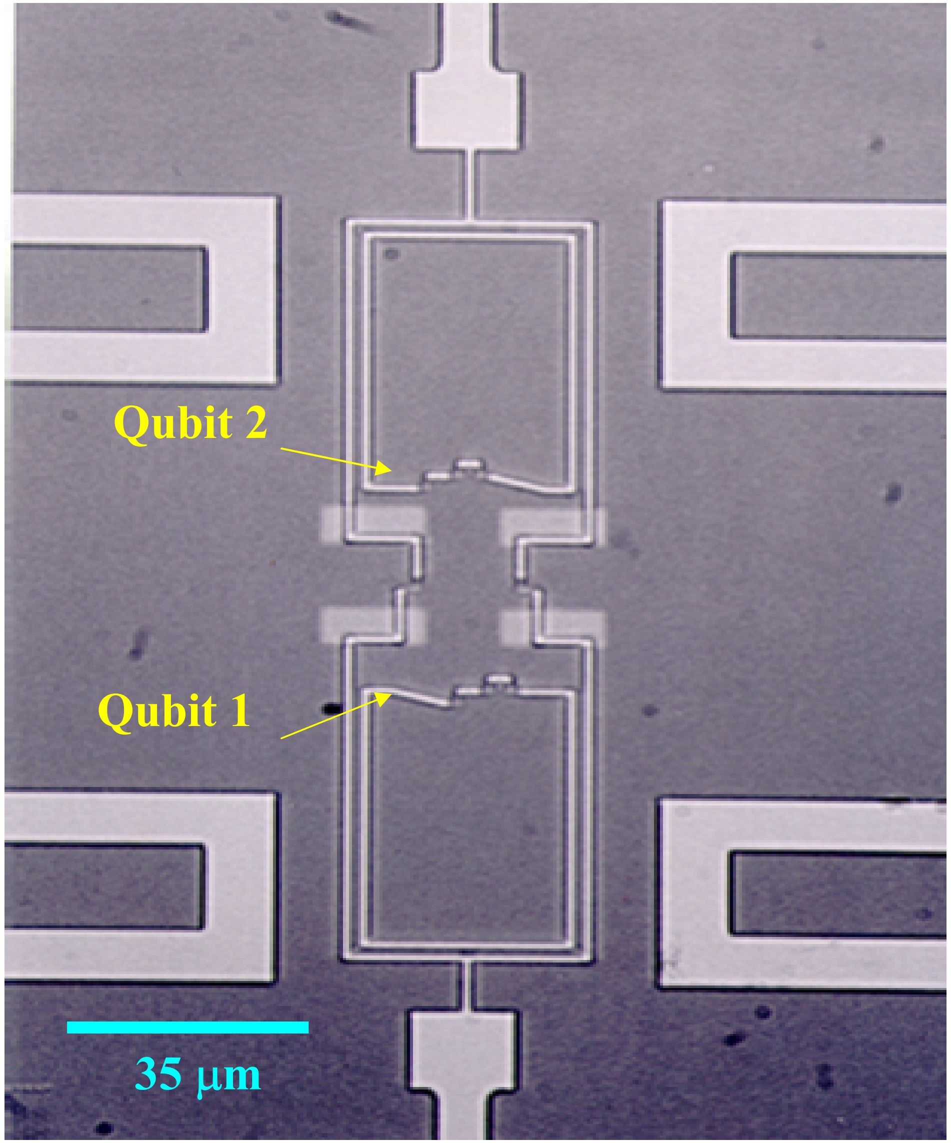

CardioMag Imaging System for Magnetocardiography

Neuromag® 306-Channel SQUID System

The Sorting Hat

"There is nothing hidden in your head
The Sorting Hat can't see,
So try me on and I will tell you
Where you ought to be."

The Science of Harry Potter

Roger Highfield, 2002

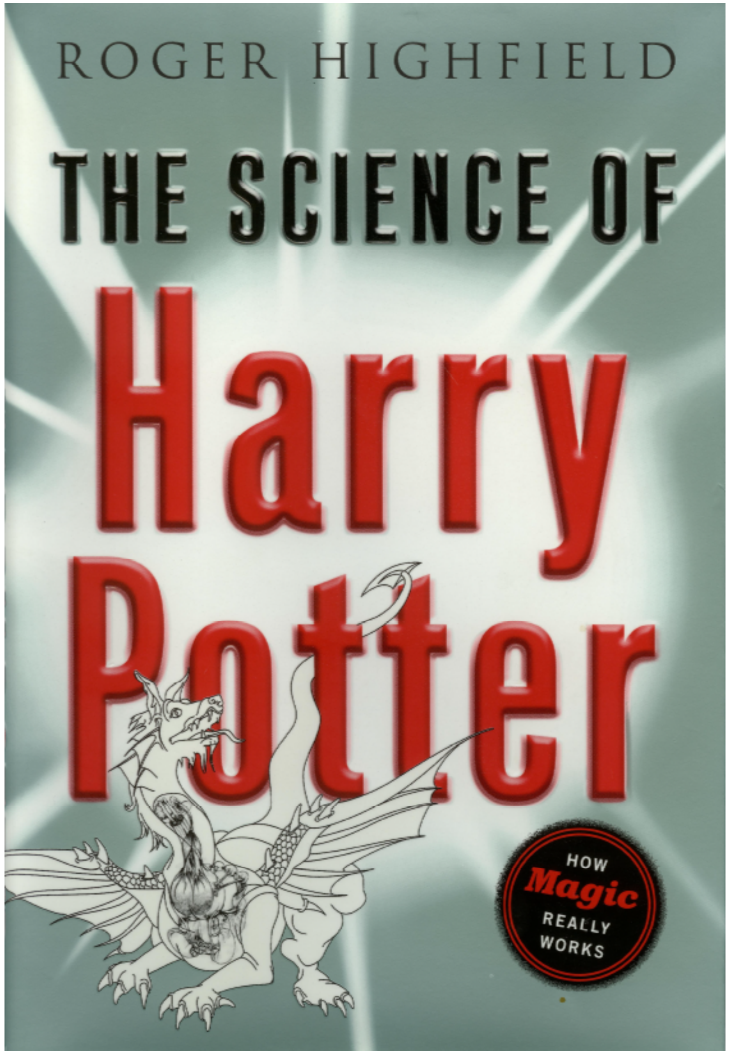

"The magnetic fields sprouting from Harry's head influence the electron pairs circulating in the SQUIDs in the Sorting Hat. Because quantum mechanics says that all the electron pairs in each SQUID act in concert (in the jargon, all the electrons are in the same "quantum state"), they convert a tiny change in his brain's magnetic field into a detectable change in voltage with a sensitivity unmatched by any other device."

Searching for Axions: The Microstrip SQUID Amplifier

University of Gießen
Michael Mück
Jost Gail
Christoph Heiden†

UCB, LBNL and LLNL
Marc-Olivier André
Darin Kinion
Jan Kycia

Support: DOE/BES
DOE/HEP
NSF

Cold Dark Matter

- Recent cosmic microwave background measurements indicate that ~25% of the mass of the universe is cold dark matter (CDM)

- A candidate particle is the axion, proposed in 1978 to explain the absence of a measurable neutron electric dipole moment

  Density of CDM: $\rho_{CDM} \approx 0.3 - 0.45$ GeV cm^{-3}

  Predicted axion mass: $m_a \approx 1\mu$eV - 1 meV (0.24 - 240 GHz)

  For $m_a = 1\mu$eV: $n_a \approx (3 - 4.5) \times 10^{14}$ cm^{-3}

Resonant Conversion of Axions into Photons

Pierre Sikivie (1983)

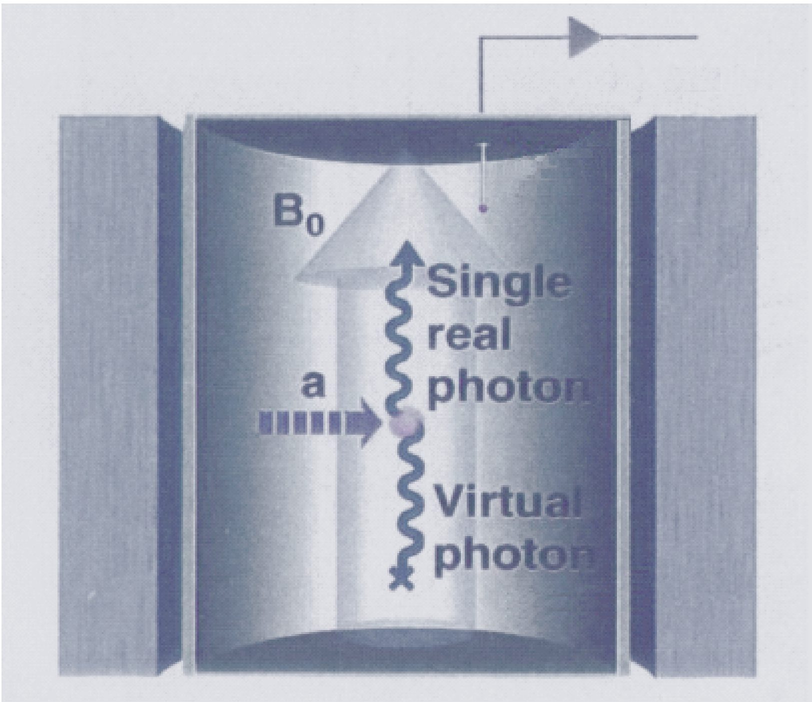

Expected Signal

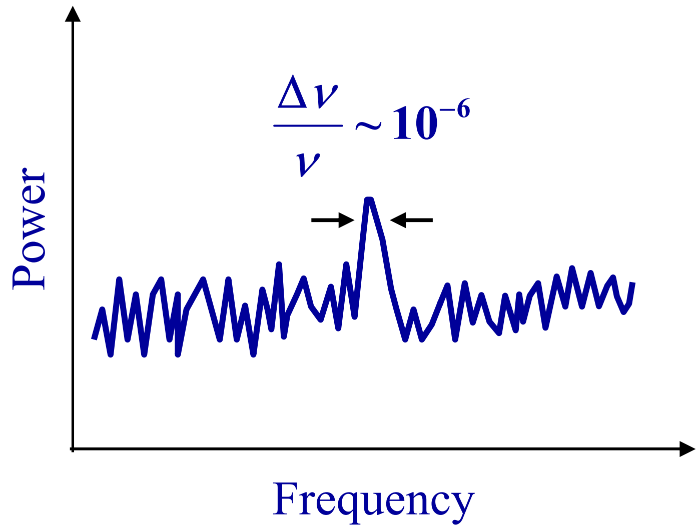

Axion Detector at
Lawrence Livermore
National Laboratory

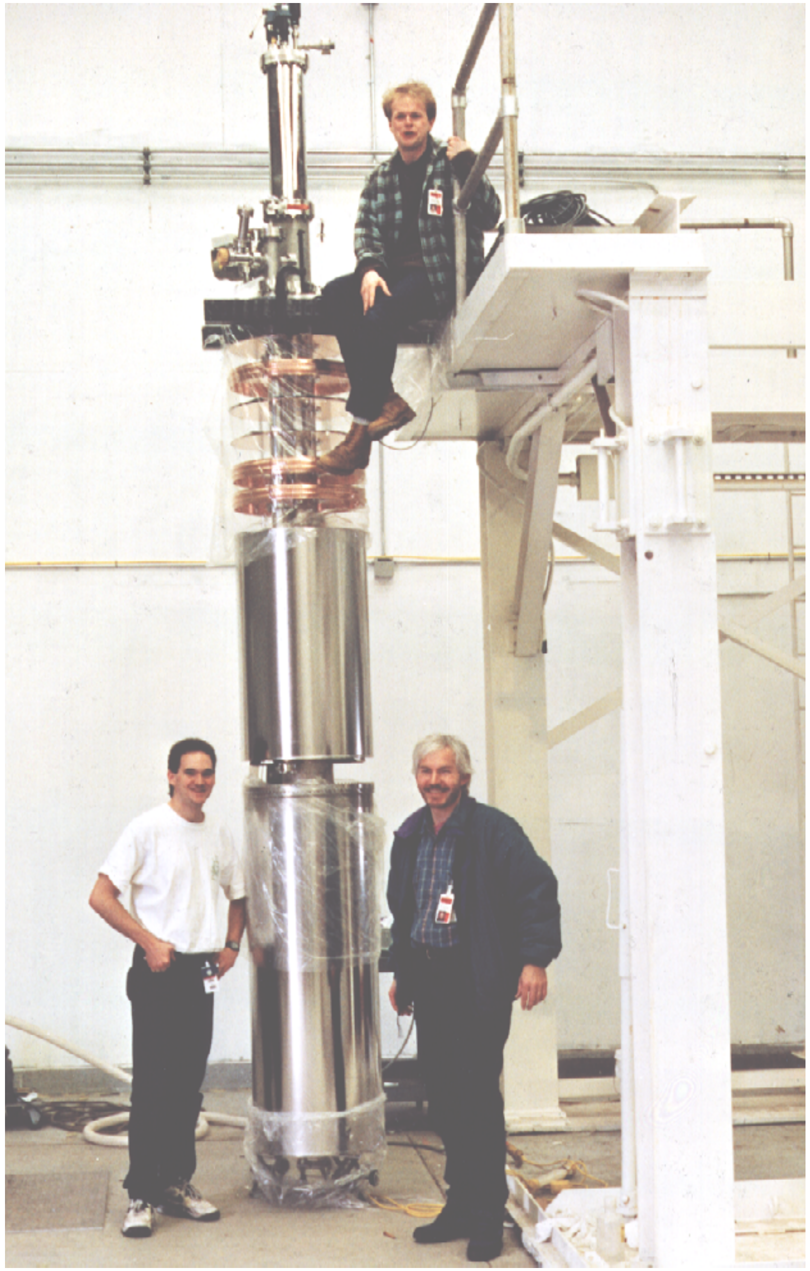

Noise Temperature

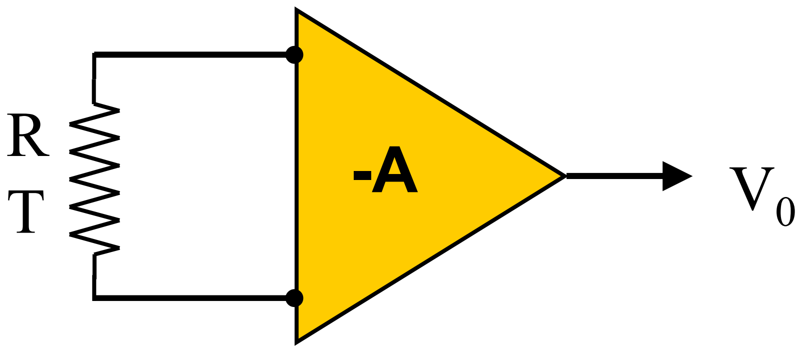

$$S_V^0(f) = A^2 \cdot 4k_B \left[T + T_N(R)\right]R$$

LLNL Axion Detector

- Current system noise temperature: $T_S = T + T_N \approx 3.2$ K

  Cavity temperature: $T \approx 1.5$ K

  Amplifier noise temperature: $T_N \approx 1.7$ K

- Time* to scan the range of frequencies from f_1 to f_2:

  $\tau(f_1, f_2) \approx 4 \times 10^{16}(T_S/1\ \mathrm{K})^2(1/f_1 - 1/f_2)$ sec

  For $f_1 = 0.24$ GHz, $f_2 = 2.4$ GHz: $\tau \approx 45$ years

- Note: There is only a factor of 2 to be gained in T_S by reducing T unless T_N is also reduced.

*Dine-Fischler-Srednicki-Zhitnitsky (DFSZ) theory

SQUID Amplifier

Top View

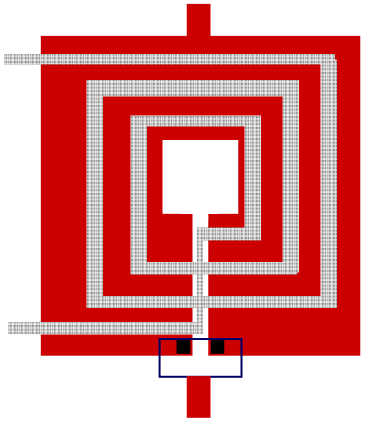

Side View

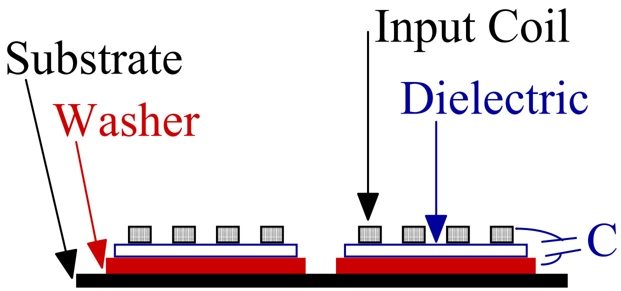

- **At high frequencies, most of the current flows through the parasitic capacitance rather than the inductance**

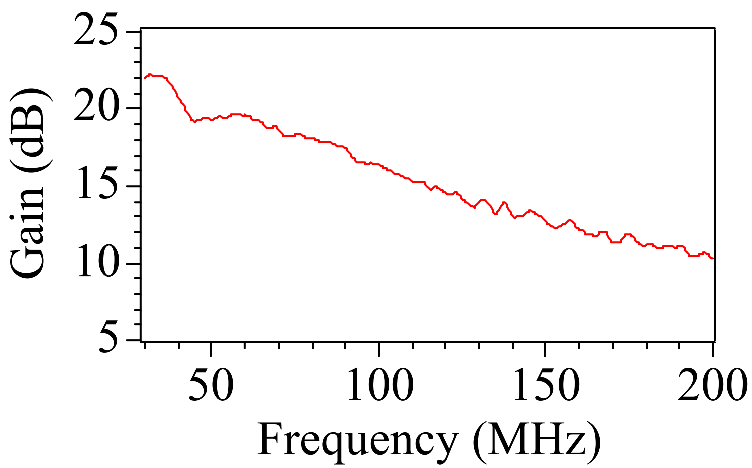

- **This reduces the gain significantly**

Microstrip SQUID Amplifier

Conventional SQUID Amplifier

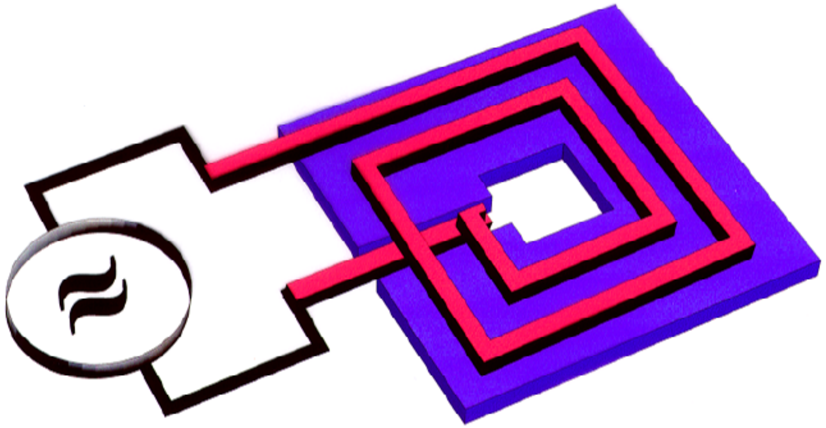

- Source connected to both ends of coil

Microstrip SQUID Amplifier

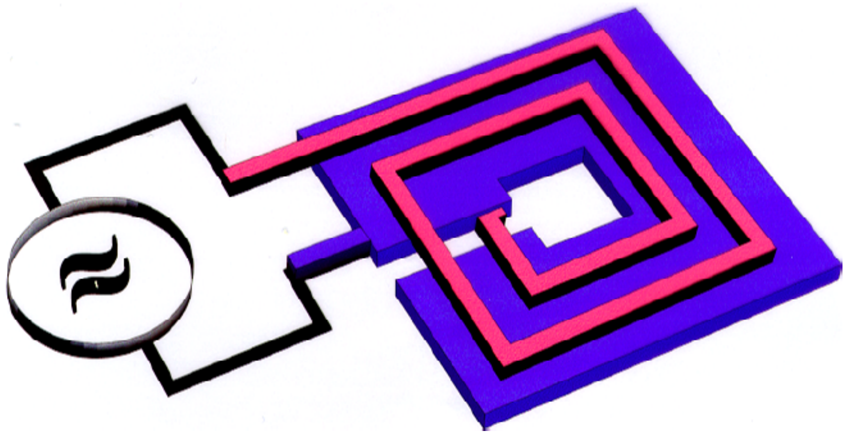

- Source connected to one end of the coil and SQUID washer; the other end of the coil is left open

Gain Measurements

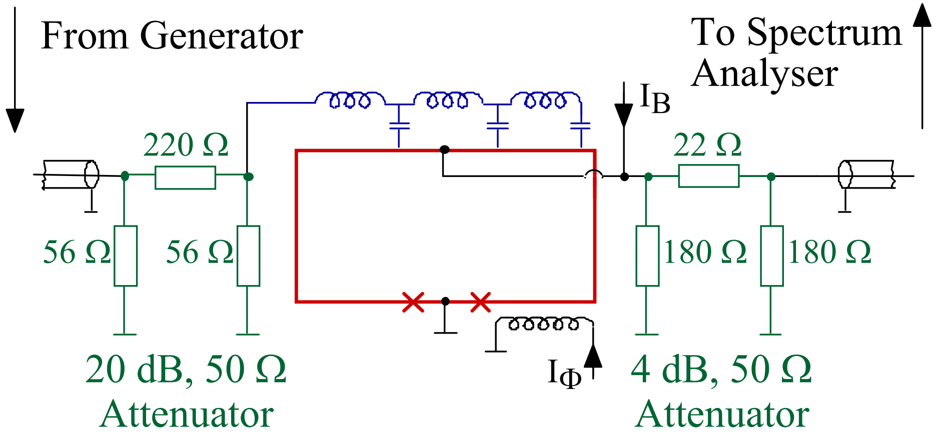

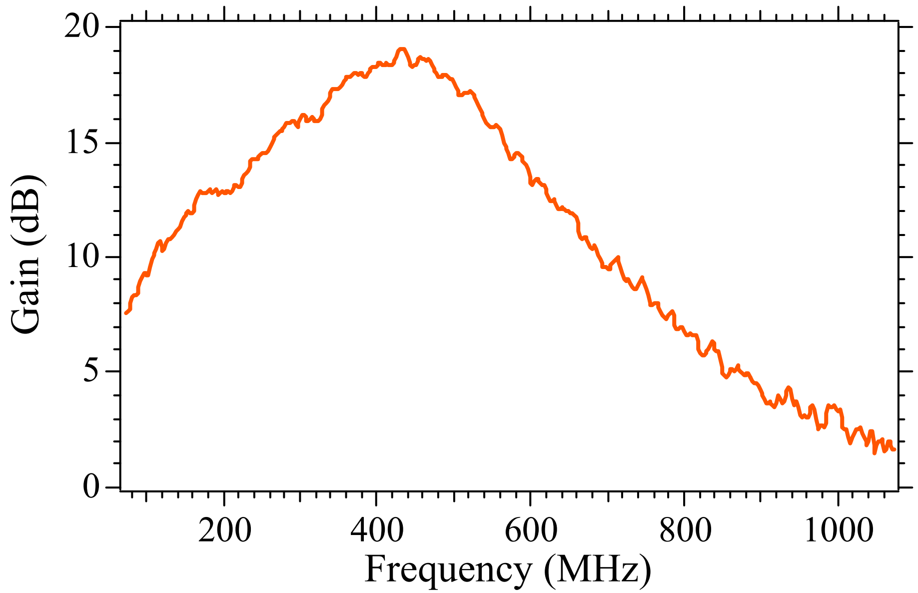

- **Gain of 11-turn microstrip SQUID with the washer grounded**

Gain vs. Coil Length

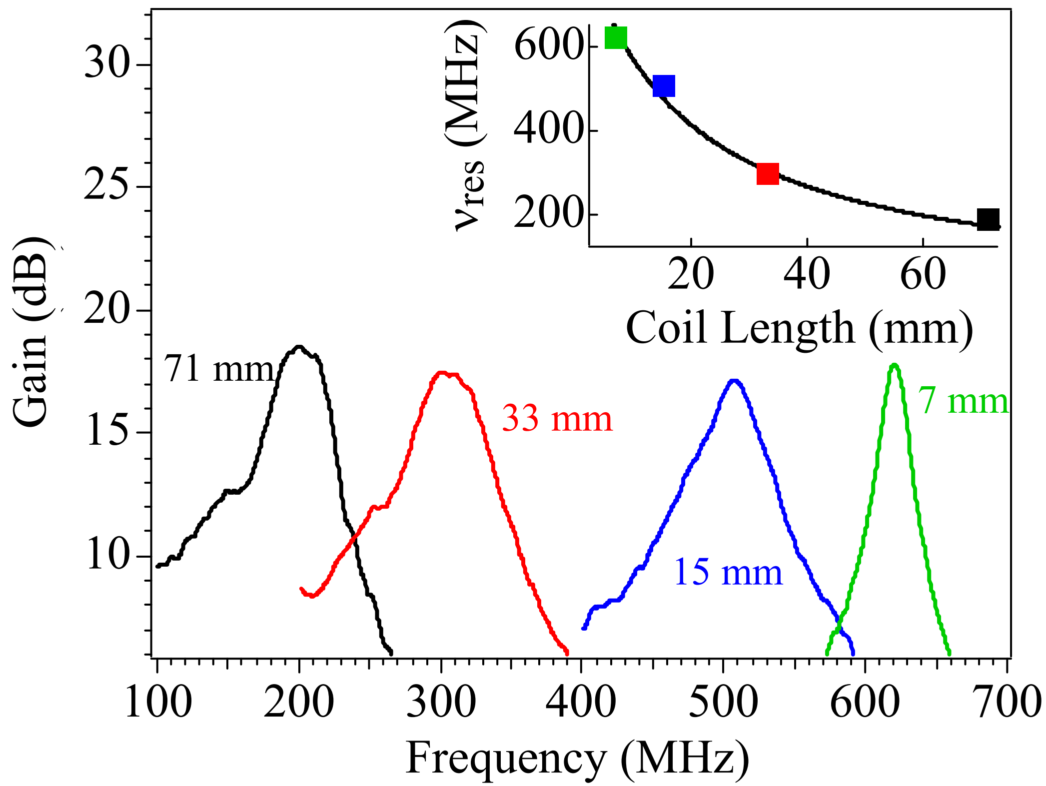

Varactor Tuning of Microstrip SQUID

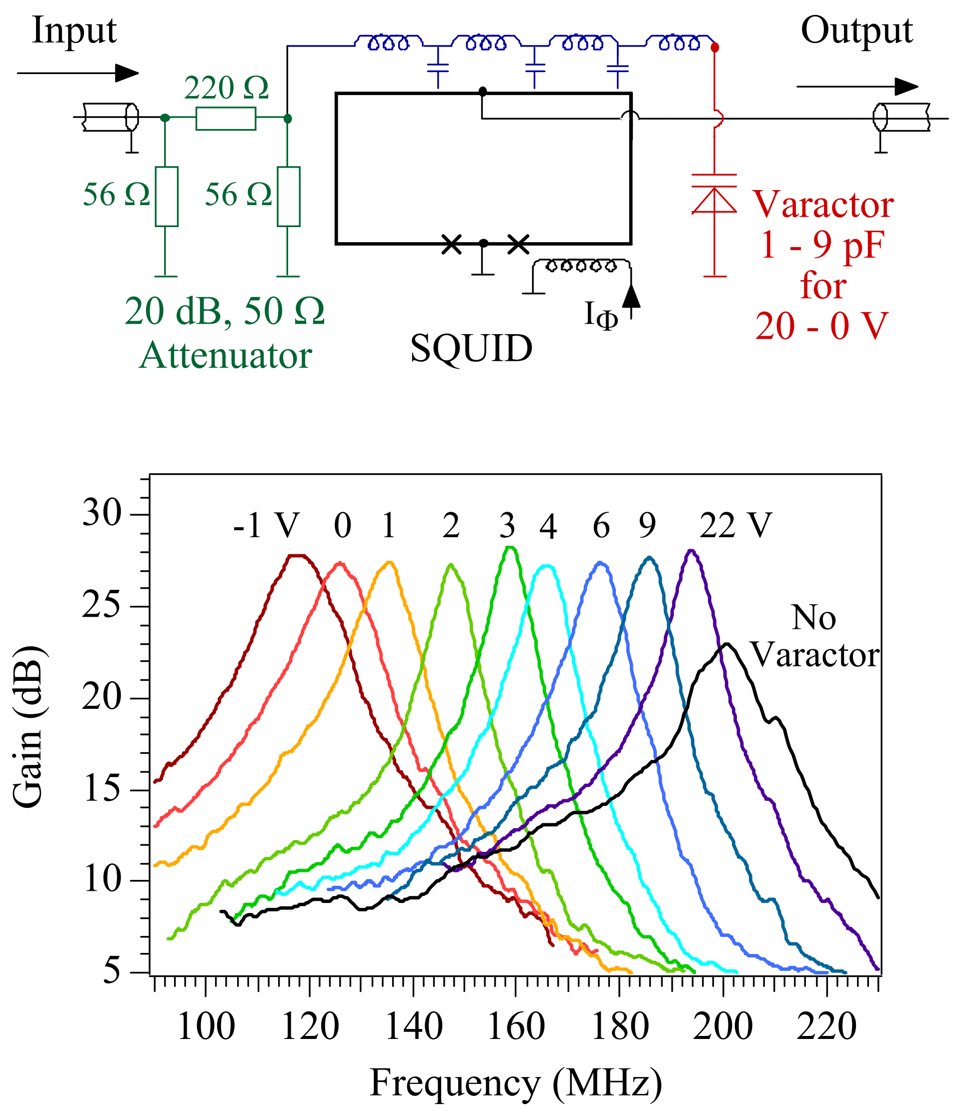

Noise Measurements at mK Temperatures

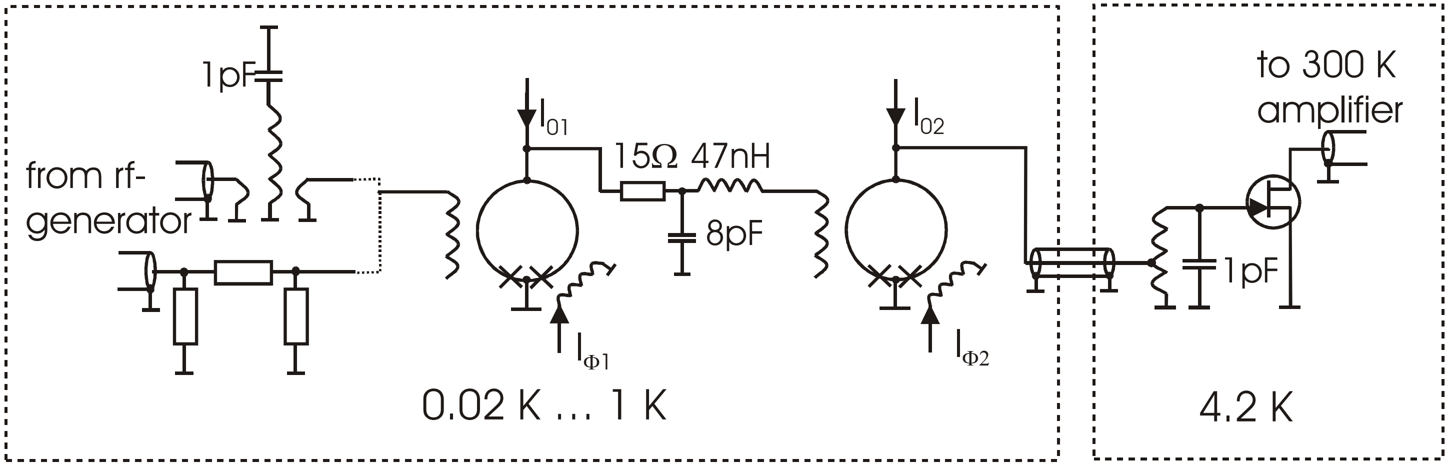

Noise Temperature at 519 MHz vs. Bath Temperature

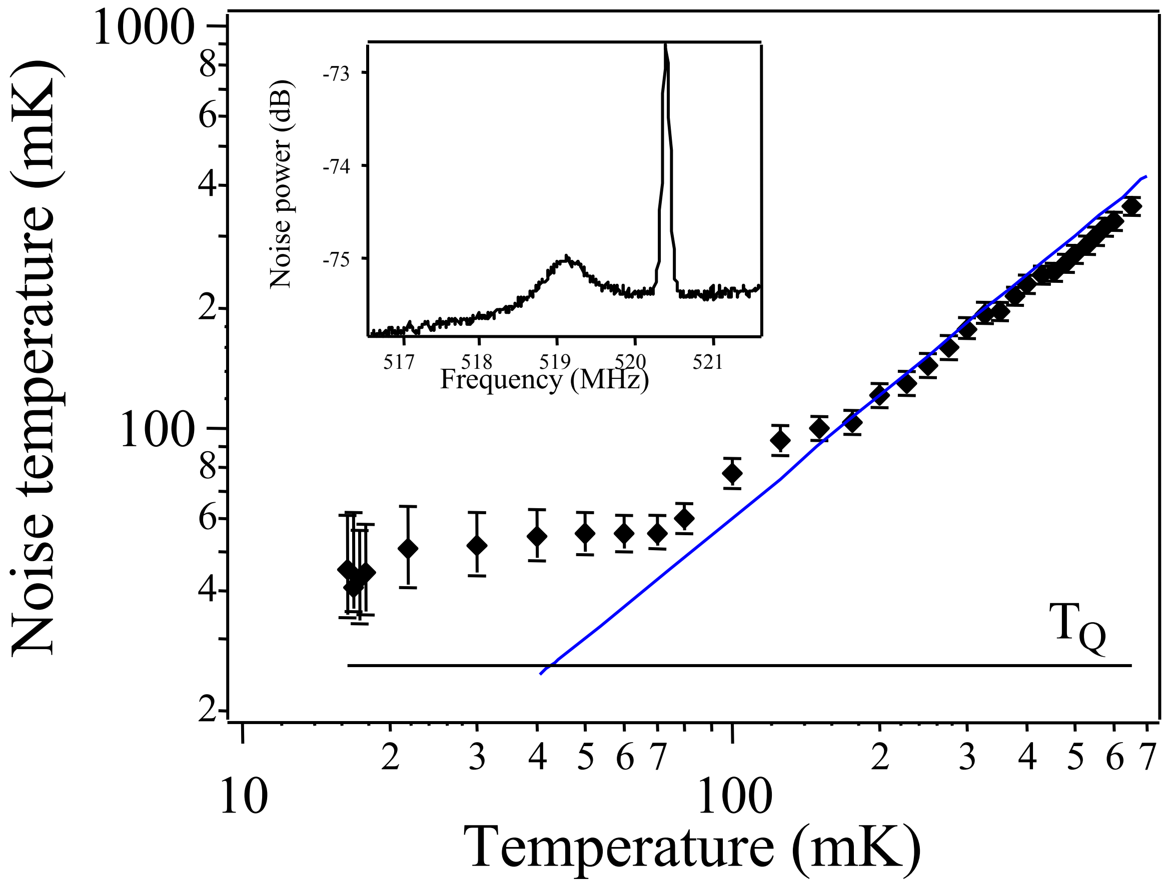

$T_N \rightarrow 47 \pm 10$ mK

$T_Q = hf/k_B \approx 25$ mK

Microstrip SQUID Amplifier: Impact on Axion Detector

- Current LLNL axion detector: $T_S \approx 3.2$ K
- For $T \approx T_N \approx 50$ mK: $T_S \approx T + T_N \approx 100$ mK

$\tau \approx 45$ years x $(0.1/3.2)^2$

≈ 18 days

Summary

- Gain ≥ 20 dB for frequencies ≤ 1 GHz
- Frequency is tunable over factor of 2 with varactor diode
- Cooled to 20 mK, T_N is within a factor of 2 of the quantum limit
- Noise temperature 40 times lower than state-of-the-art cooled semiconductor amplifiers

Future directions

- Install microstrip SQUID amplifier on the axion detector at 4.2 K to demonstrate proof-of-principle (Fall 2006)
- Implement second-generation axion detector at 50mK: expected to increase scan rate by three orders of magnitude

Microtesla Nuclear Magnetic Resonance and Magnetic Resonance Imaging

- Nuclear magnetic resonance
- Why use a SQUID?
- Magnetic resonance imaging

Michael Hatridge
Nathan Kelso
SeungKyun Lee
Robert McDermott
Michael Mössle
Michael Mück
Whit Myers
Bennie ten Haken
Andreas Trabesinger
Erwin Hahn
Alex Pines

Nuclear Magnetic Resonance

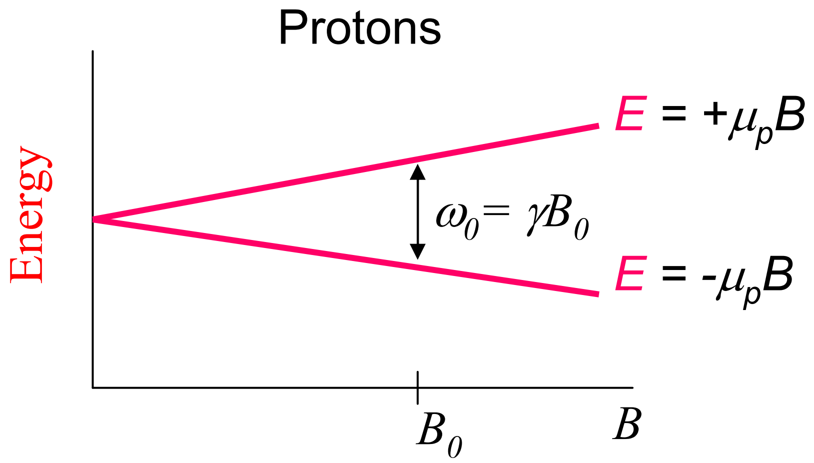

$\nu_0 = 42.58$ MHz/tesla

γ **gyromagnetic ratio**

Magnetic moment ($\mu_p B_0 << k_B T$):

$$M = N\mu_p \frac{N_\uparrow - N_\downarrow}{N_\uparrow + N_\downarrow} = \frac{N\mu_p^2 B_0}{k_B T}$$

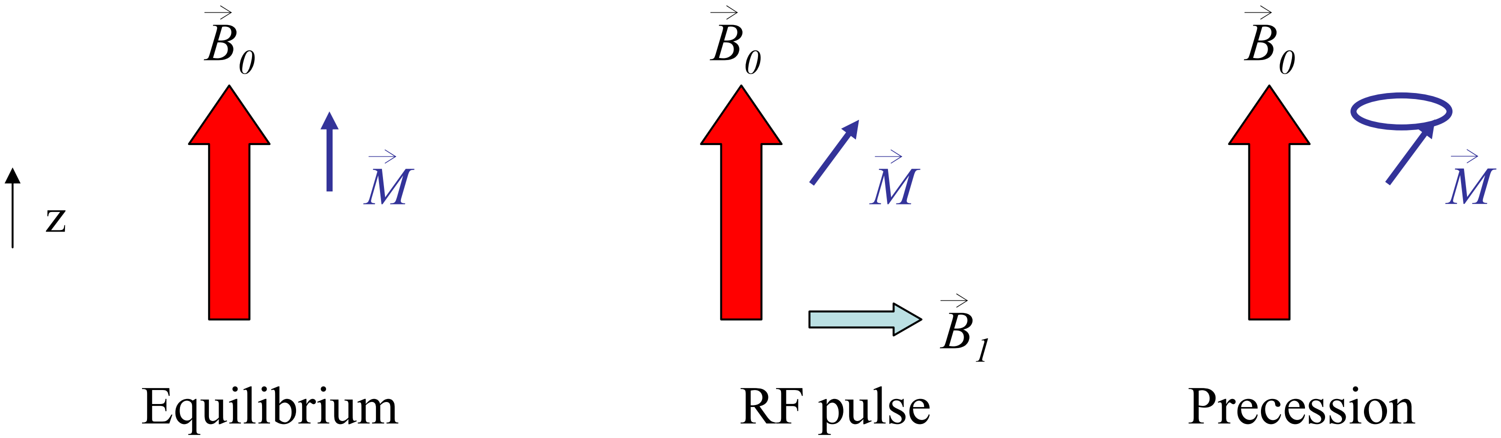

Spin Echo

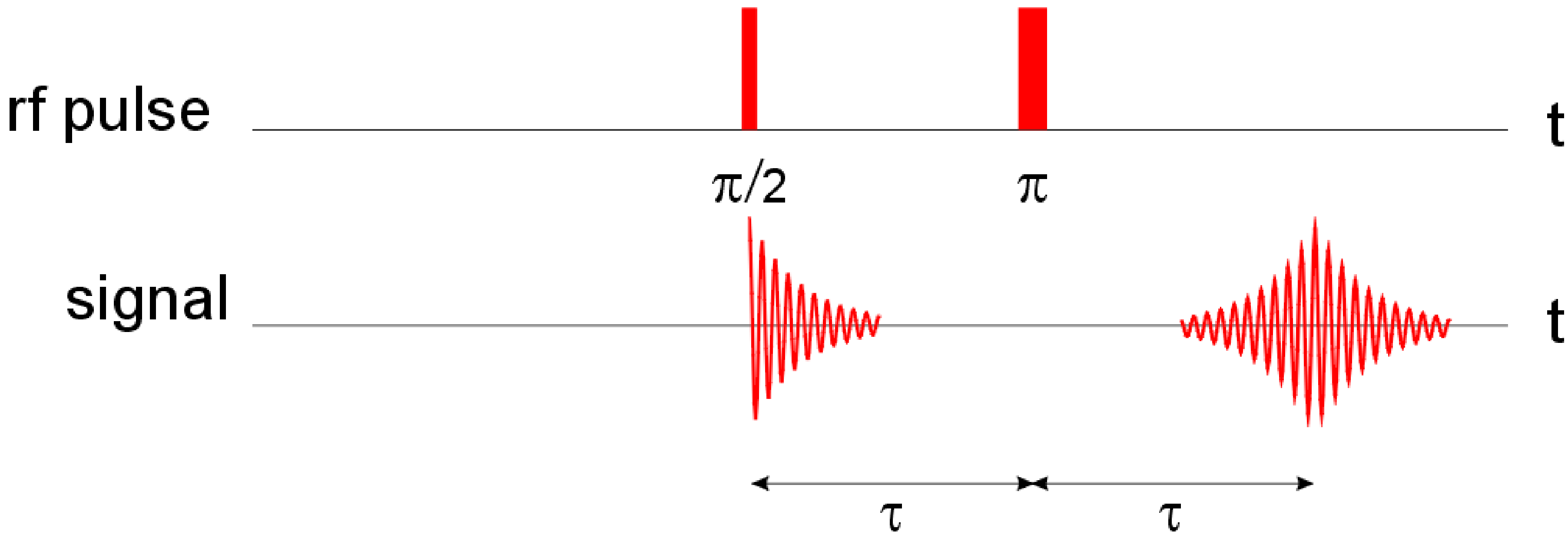

Relaxation Processes in NMR

- Longitudinal (spin-lattice) relaxation time T_1
  - Microseconds to weeks
  - After spins are excited, polarization returns to equilibrium (along longitudinal axis) by emitting quanta: spin-flip process

- Transverse (spin-spin) relaxation time T_2
  - Time for precessing spins to dephase ("homogeneous broadening")

- Inhomogenous lifetime T_2'
  - Magnetic field inhomogeneity broadens the line ("inhomogeneous broadening")

- Linewidth: $\Delta f = 1/2\pi T_2^*$

  where $1/T_2^* = 1/T_2 + 1/T_2'$

NMR Linewidths in Liquids

- Narrow (~1Hz) linewidths desirable: high resolution NMR spectroscopy
  high spatial resolution MRI

- Linewidths broadened by magnetic field inhomogeneities:
  - inherent in coils
  - environmental magnetic susceptibility inhomogeneity
  - sample magnetic susceptibility inhomogeneity

- Inhomogeneous linewidth for field change ΔB across sample:

  $\Delta f = (\gamma/2\pi)\,\Delta B = (\gamma/2\pi)(\Delta B/B)B \propto B$ for given *relative* inhomogeneity $\Delta B/B$

- High-field NMR magnets (~20T) require "shimming" to a field homogeneity of 1 part in 10^9 to achieve 1 Hz linewidth.

- In low fields (~ Earth's field, 50 μT), a 1 Hz linewidth requires a homogeneity of 1 part in 2000.


BRUKER
900
UltraStabilized™
BRUKER

NMR: Faraday coil vs. SQUID

Conventional high-field NMR

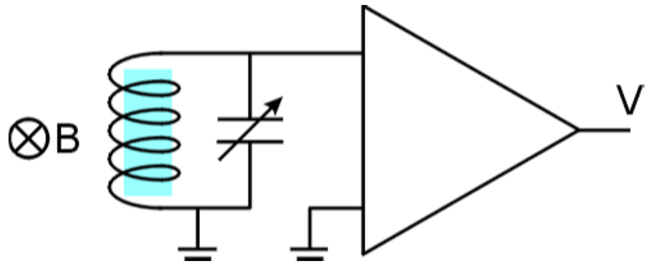

$M \propto \mu_p B_0 / k_B T$

$V \propto dM / dT \propto \omega_0 B_0$

$\propto B_0^2$

Exquisite field homogeneity required to achieve high spatial resolution

SQUID low-field NMR

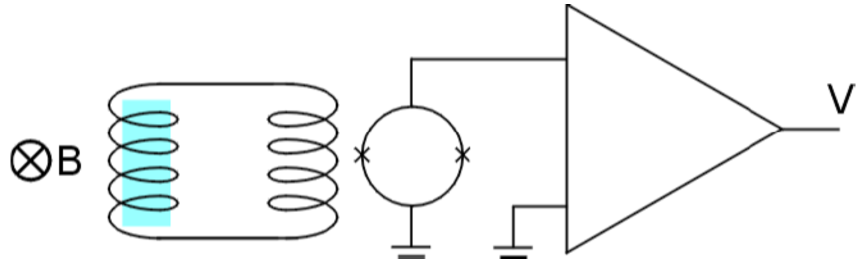

$M \propto \mu_p B_0 / k_B T$

$V \propto M$

$\propto B_0$

Field homogeneity requirements are modest

Prepolarization of spins at $B_p > B_0$:
M is independent of B_0
V is independent of B_0

Cryogenic Configuration

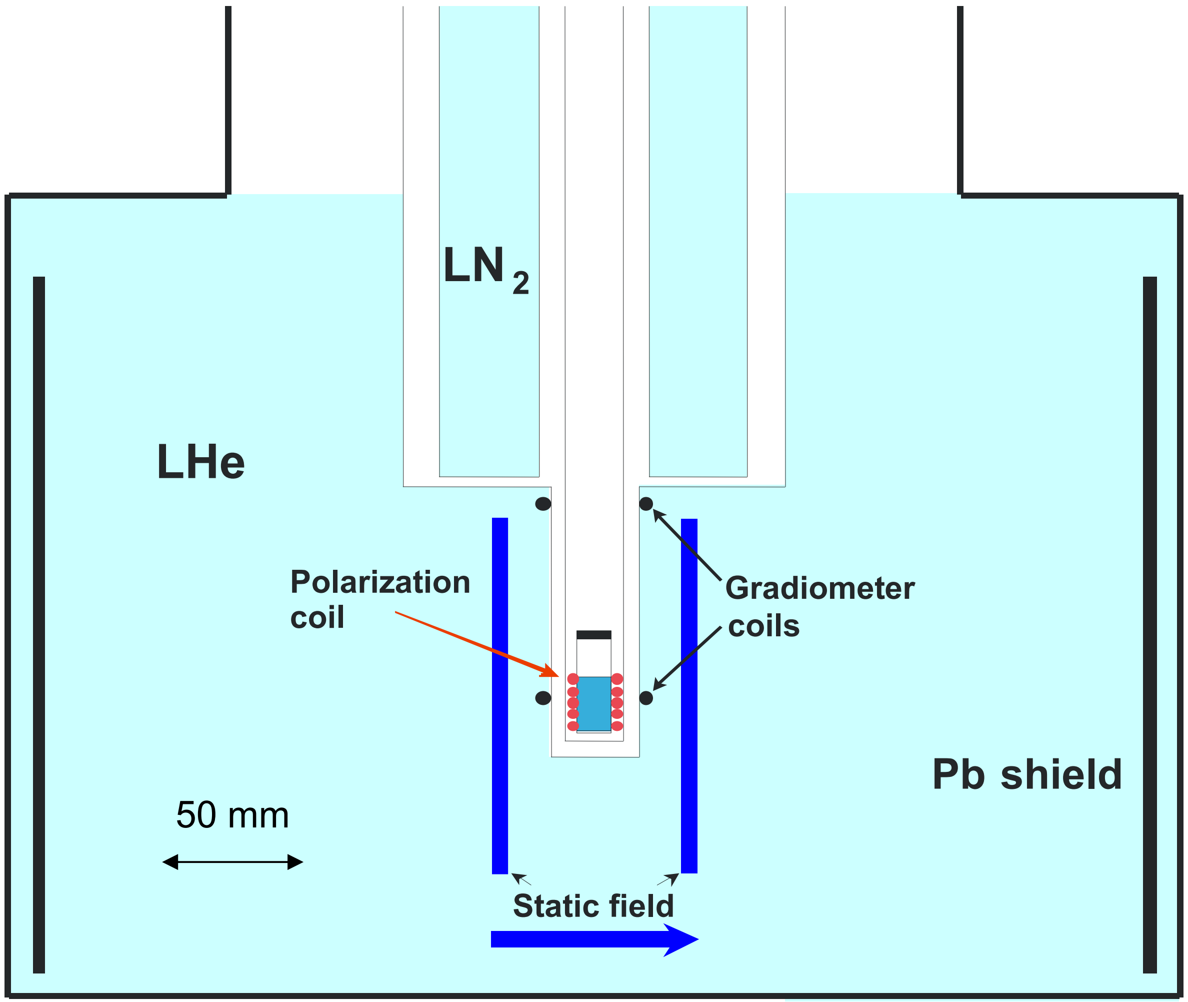

Narrowed Linewidths and Enhanced Signal-to-Noise Ratio

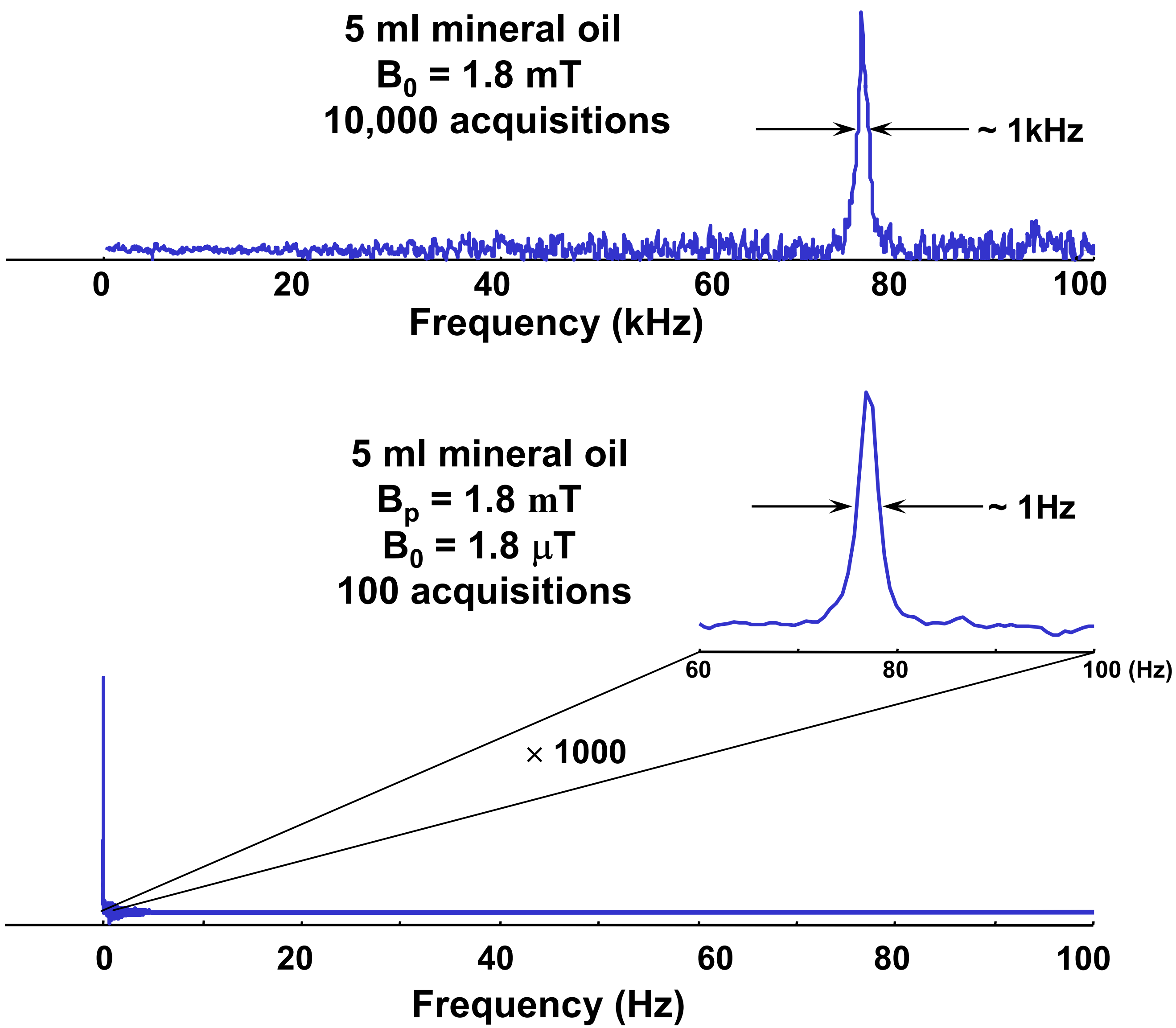

High Field MRI

3T MRI scanner (GE)

1.5T MRI scanner (GE)

Timeline

Michael Crichton, 1999

"Most people", Gordon said, "don't realize that the ordinary hospital MRI works by changing the quantum state of atoms in your body ... But the ordinary MRI does this with a very powerful magnetic field - say 1.5 tesla, about twenty-five thousand times as strong as the earth's magnetic field. We don't need that. We use Superconducting QUantum Interference Devices, or SQUIDs, that are so sensitive they can measure resonance just from the earth's magnetic field. We don't have any magnets in there".

The "Cube"

MRI Coils

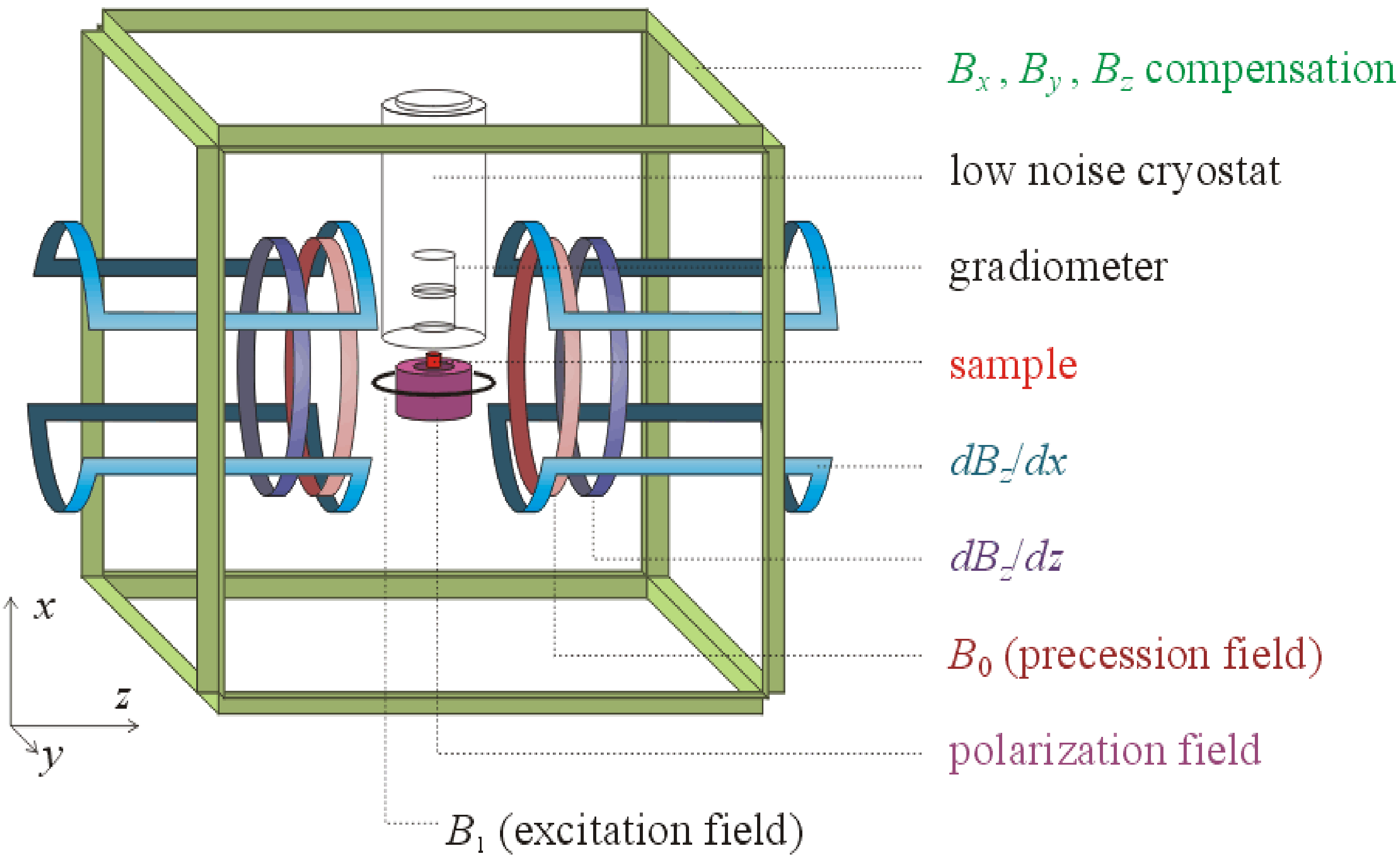

B_x, B_y, B_z compensation
low noise cryostat
gradiometer
sample
dB_z/dx
dB_z/dz
B_0 (precession field)
polarization field
B_1 (excitation field)
x
z
y

SQUID-Based Second Derivative Gradiometer

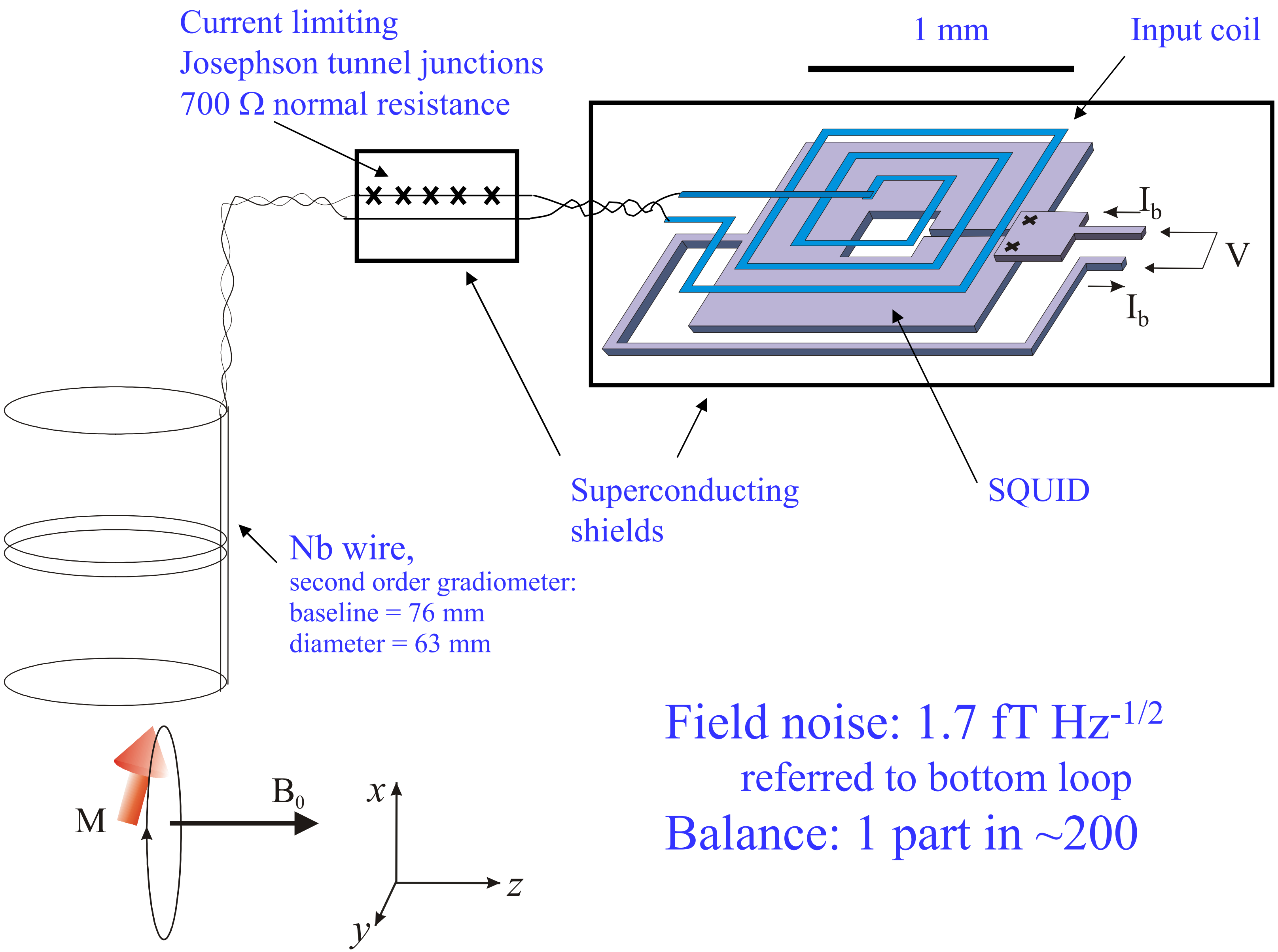

Field noise: 1.7 fT Hz$^{-1/2}$

referred to bottom loop

Balance: 1 part in ~200

Pulse Sequence for Two-Dimensional Imaging

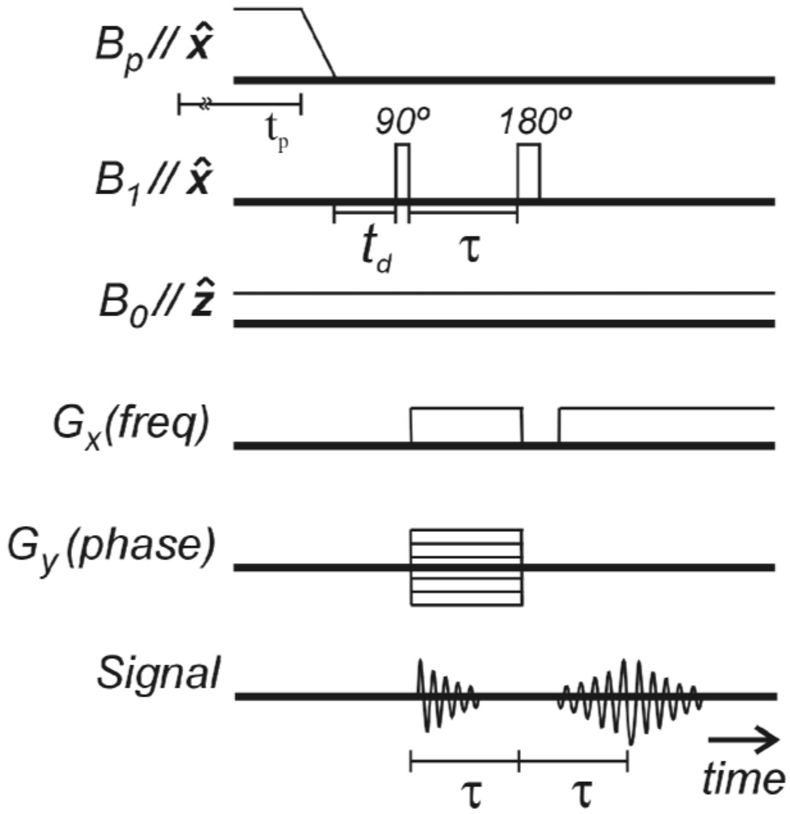

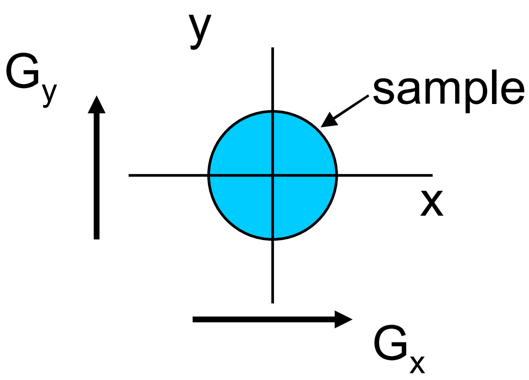

Frequency encoding:

$G_x = dB_z/dx \qquad \omega = \gamma(B_0 + xG_x)$

Phase encoding:

$G_y = dB_y/dz \qquad \Delta\phi = \gamma z G_y \tau$

$B_p = 0.3$ T, $t_{pol} = 0.1 - 2s$, $B_0 = 132\ \mu T$

Two-Dimensional Images

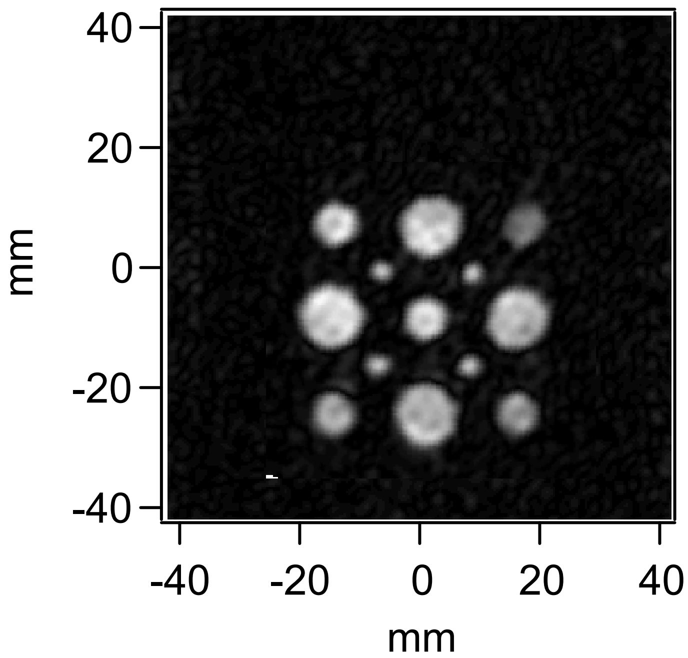

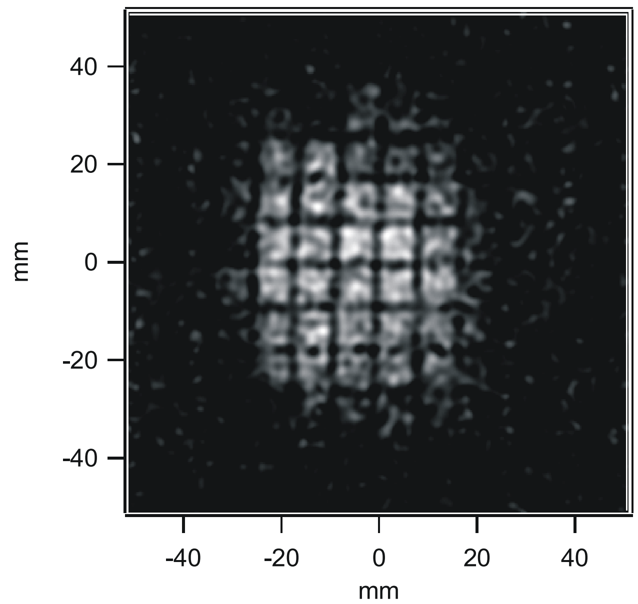

Resolution: 1.5 mm
SNR: 10
Acq. Time: 1.5 min

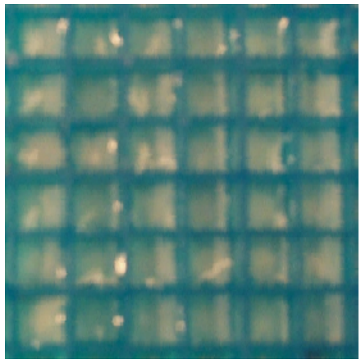

Resolution: < 1 mm
SNR: 5
Acq. Time: 5 min

Red Pepper

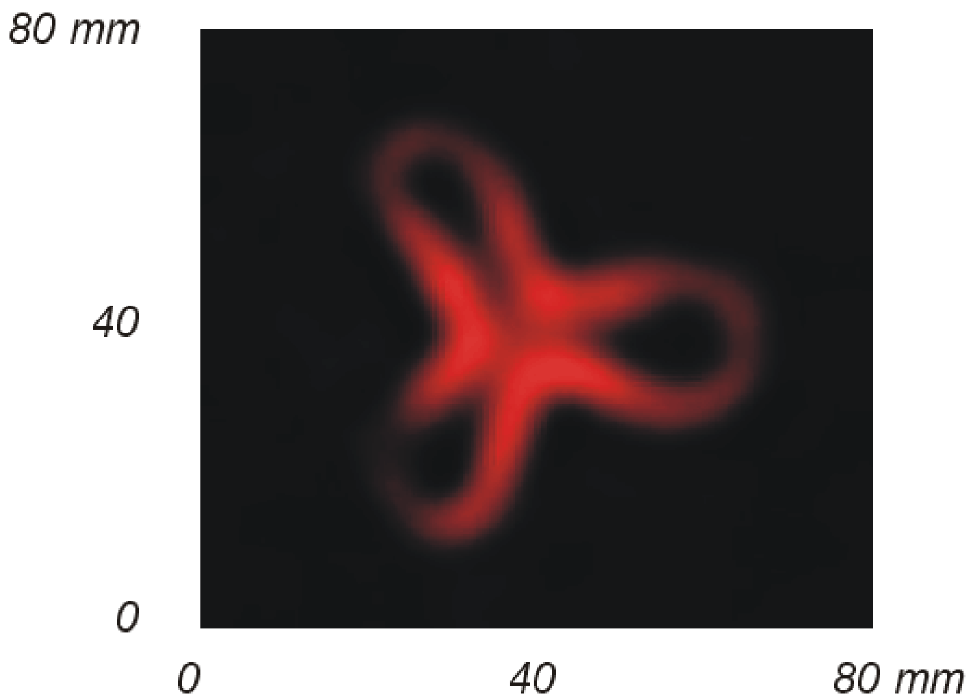

Magnetic field: 0.000132 T
NMR frequency: 5600 Hz

Corn

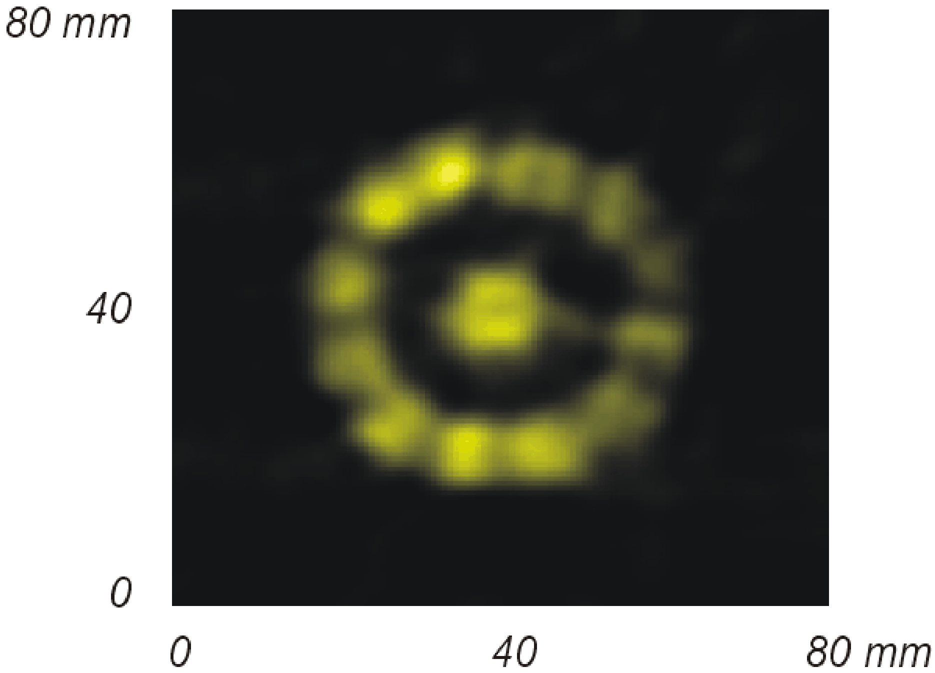

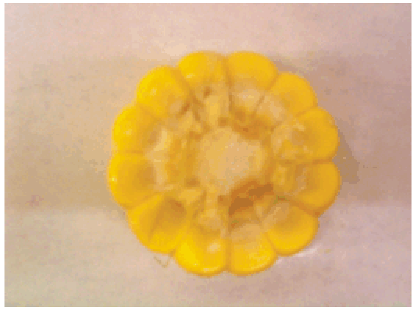

Magnetic field: 0.000132 T
NMR frequency: 5600 Hz

Three-Dimensional Images of a Pepper

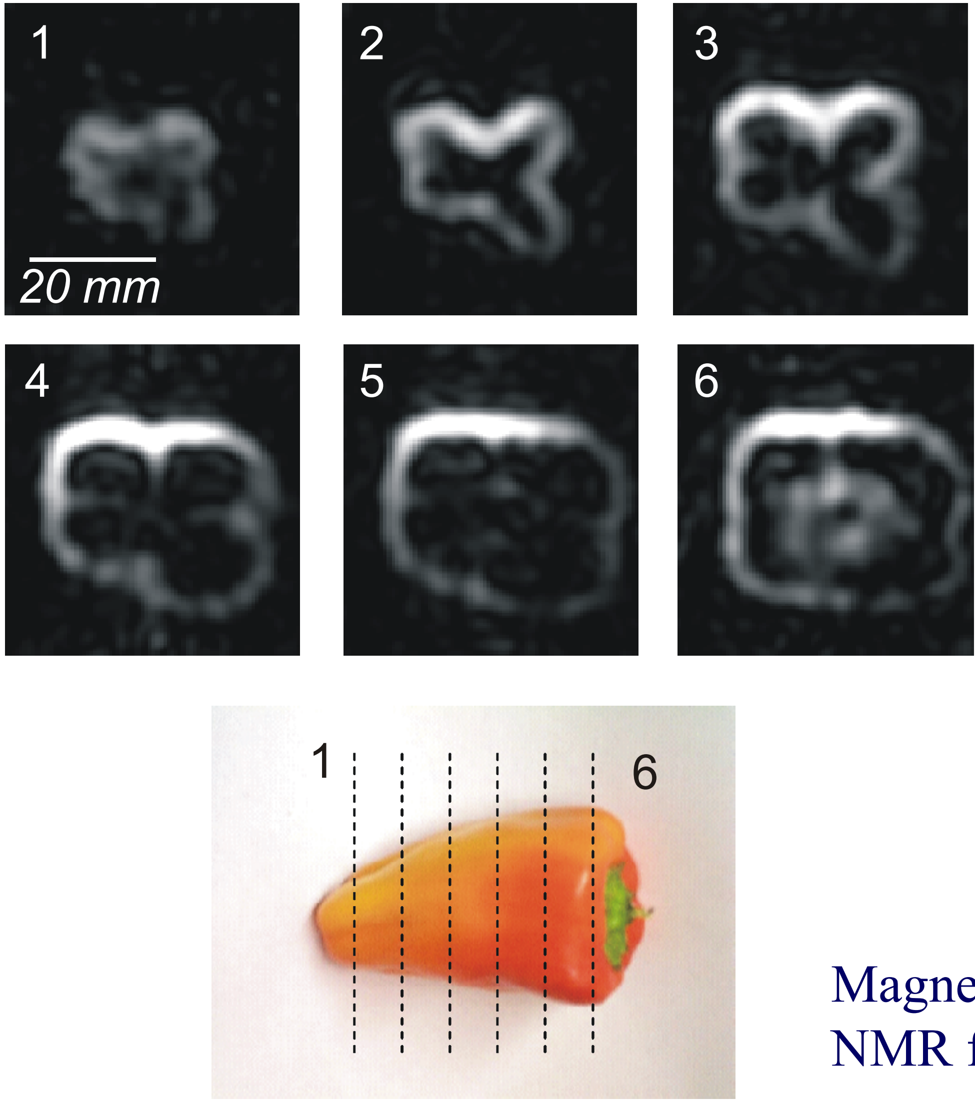

Magnetic field: 0.000132 T
NMR frequency: 5600 Hz

Image of an Arm (20 mm slice)

Subcutaneous fat

Bone marrow

Bone appears dark

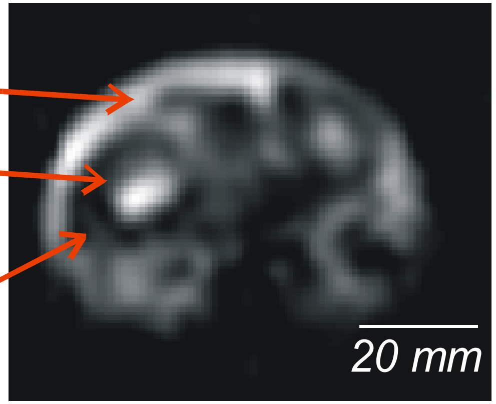

$\omega_0/2\pi$ = *5.6 kHz*

B_p = *40 mT*

Gradients: ~70 μ*T/m*

Acquisition time: 400 s

Resolution: ~3 mm

T_1-weighted Contrast Imaging

- T_1 depends strongly on the environment of the protons
- T_1-weighted contrast imaging is widely used in conventional MRI to distinguish different types of tissue
- T_1(malignant tissue) differs from T_1(normal tissue)
- T_1-contrast can be much higher in low fields

Measurement of T_1-relaxation

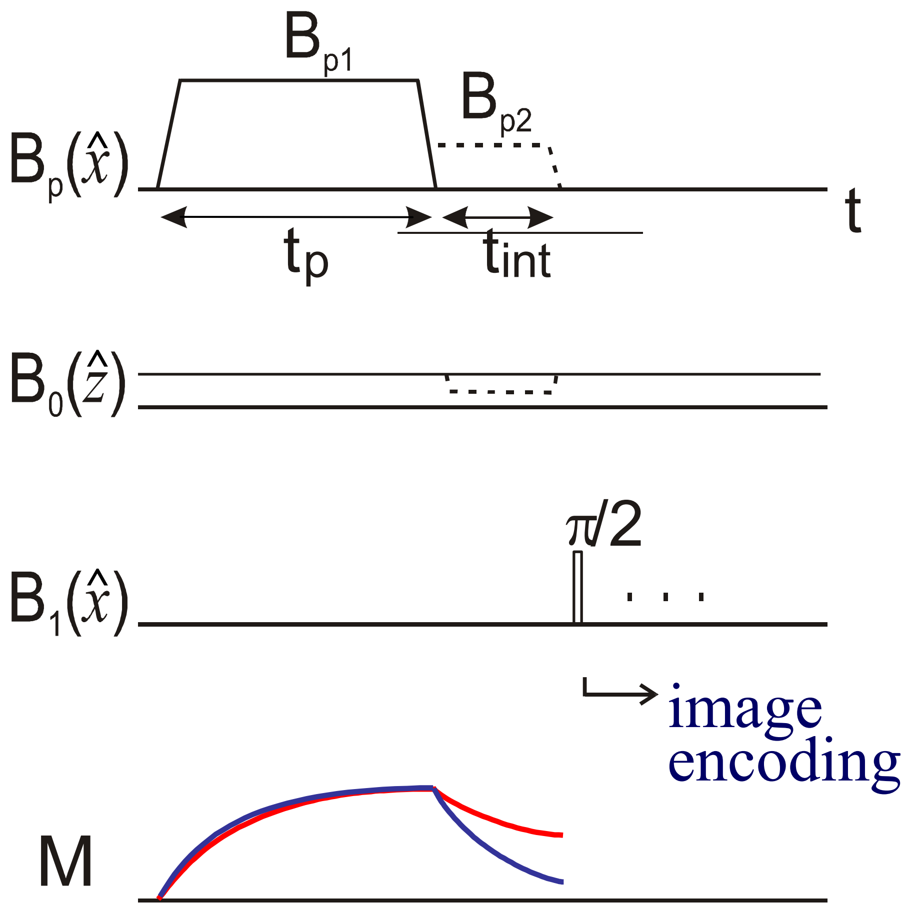

T_1 contrast images of agarose gel

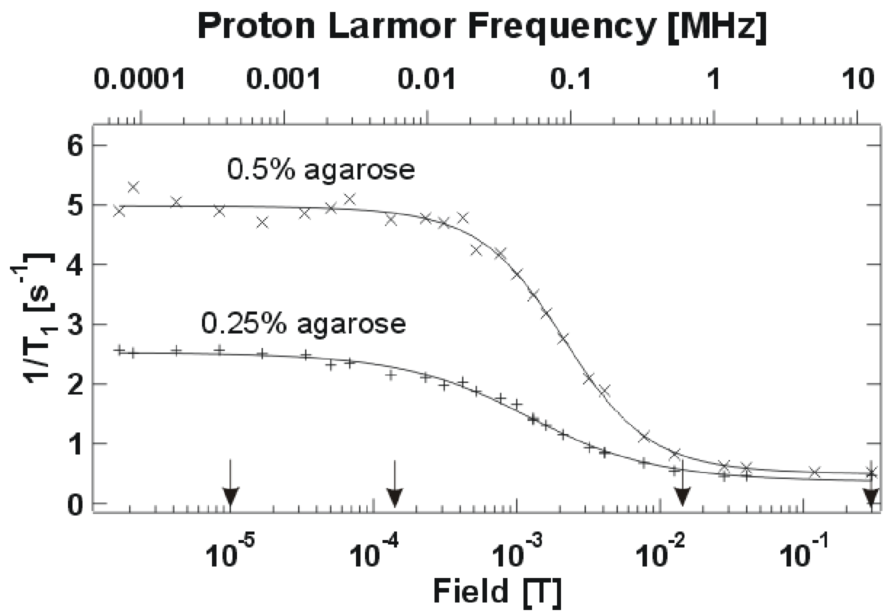

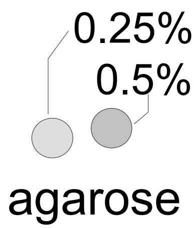

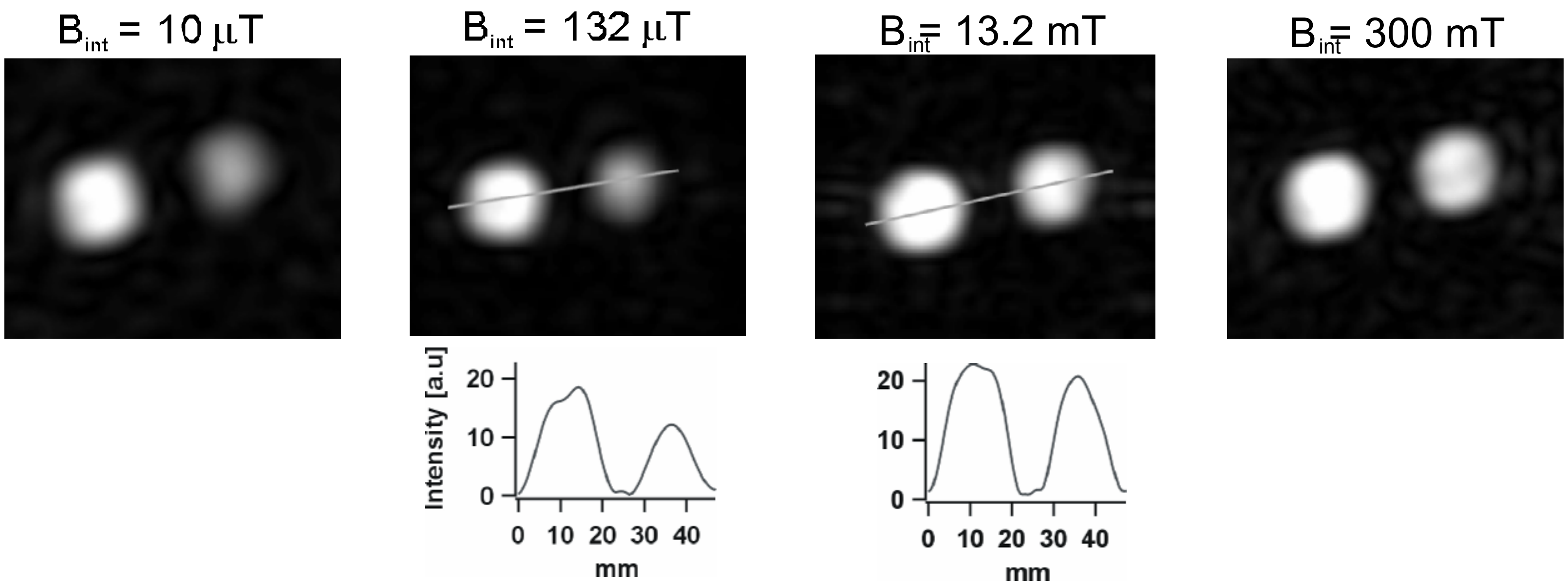

T_1-Weighted Contrast

Phantom:
Water columns in
0.5% agarose gel
Sizes: 1 mm to 6 mm

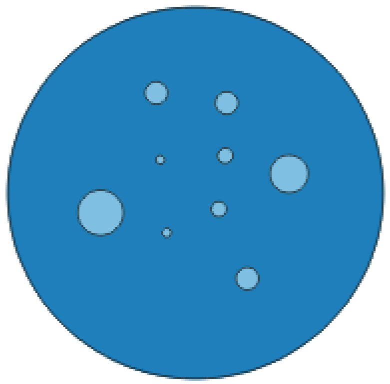

T_1-contrast at 0.1 T

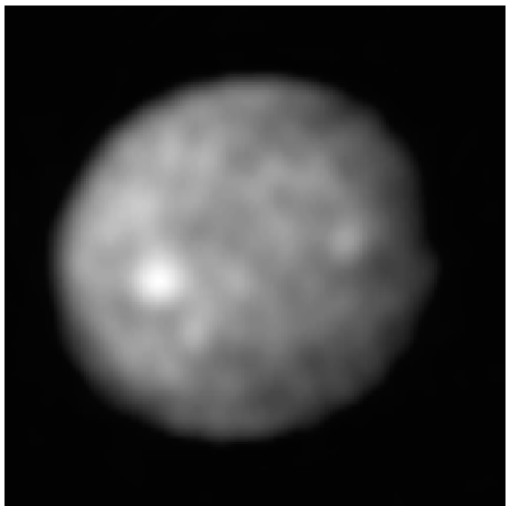

Water: $T_1 \sim 1.6$ s

Gel: $T_1 \sim 1.5$ s

T_1-contrast at 0.000132 T

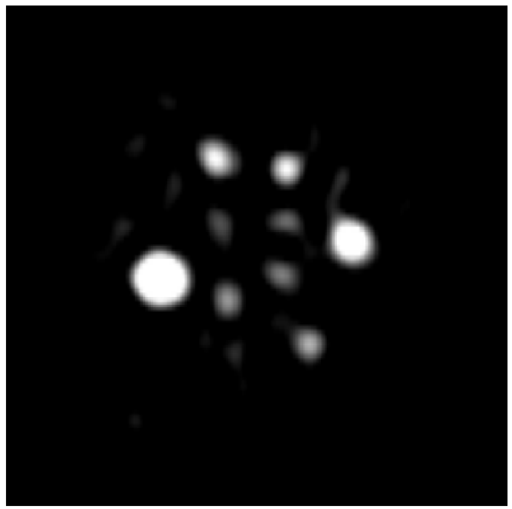

Water: $T_1 \sim 1.6$ s

Gel: $T_1 \sim 0.3$ s

Pulse Sequence for Inversion Recovery

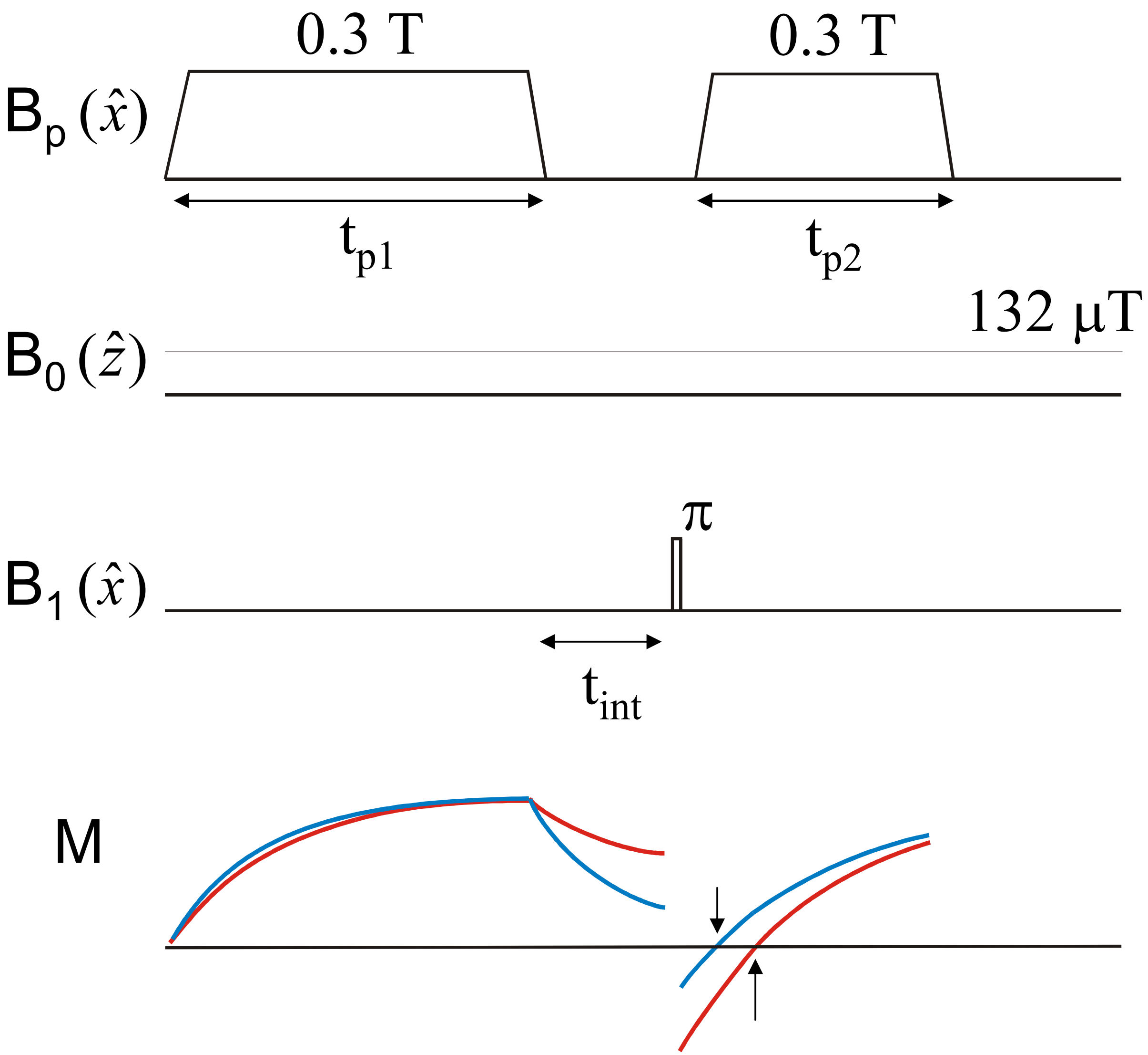

Inversion Recovery Images

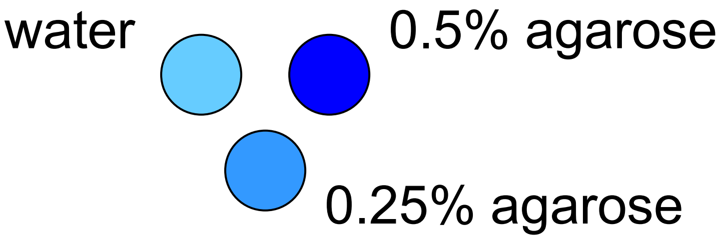

t_{p1} = 2 s
t_{int} = 200 ms

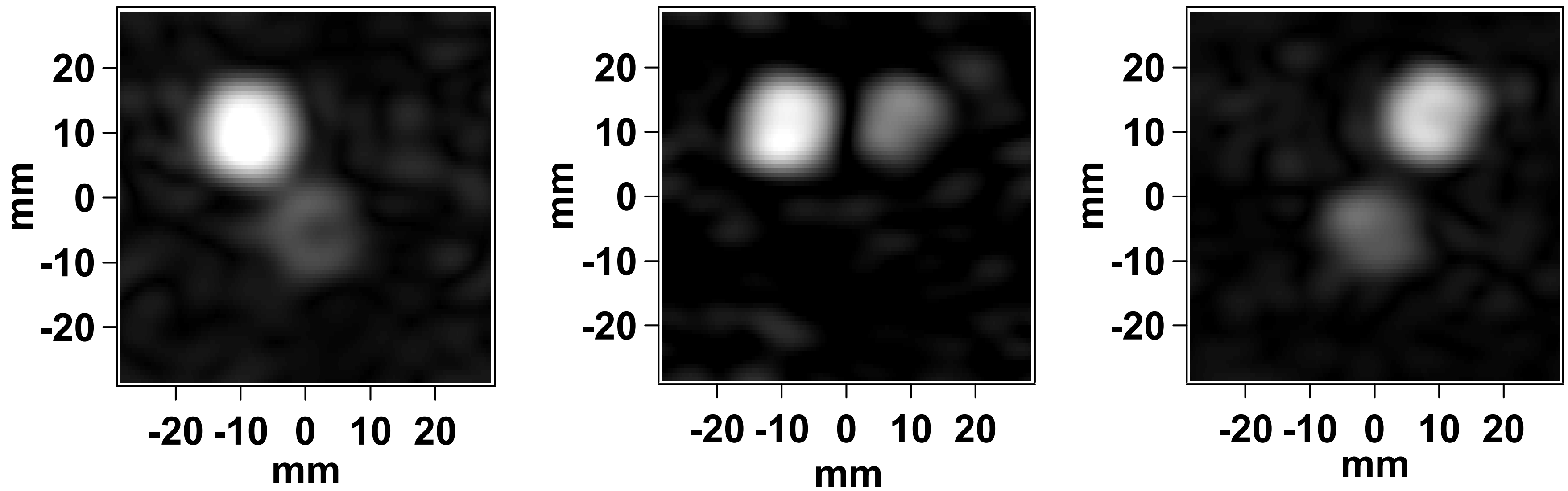

t_{p2} = 200 ms t_{p2} = 700 ms t_{p2} = 900 ms

Imaging Metal Objects

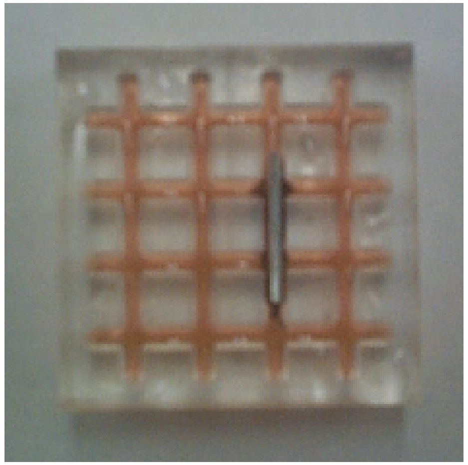

Phantom: 2-mm wide grooves filled with water containing 2-mm Ti bar

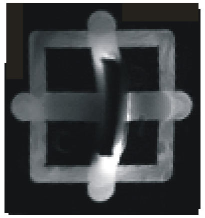

B_0=4.7 T

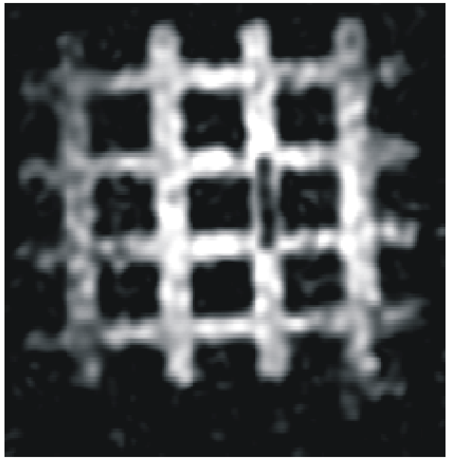

B_0=66 mT

MRI Monitoring of Freezing a Phantom

Flow liquid nitrogen through a metal tube in a water phantom

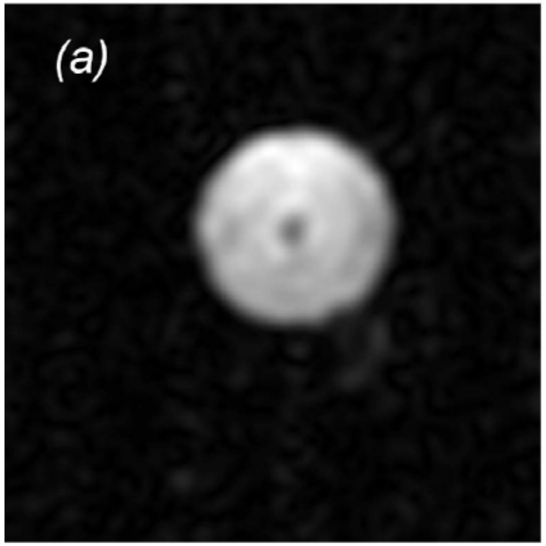

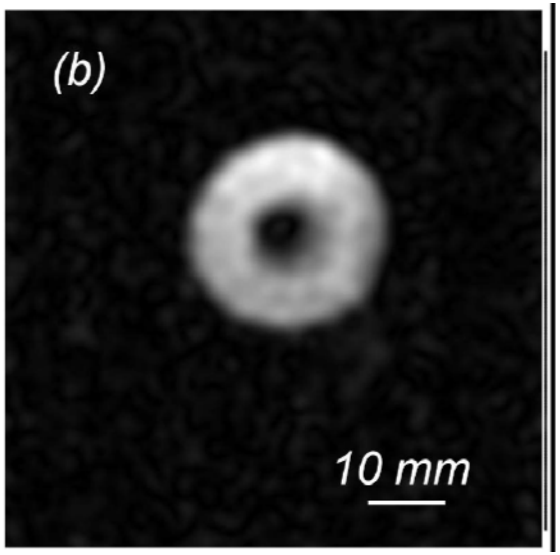

Before freezing After freezing

Potential Advantages of Microtesla MRI Compared with Conventional MRI

- Lower cost
- More open system
- Comparable spatial resolution for small parts of the body
- Improved T_1-contrast imaging
- Ability to image in the presence of metal implants and biopsy needles

BUT

- Slower
- Difficult to extend to whole body—thus less versatile

Future System Upgrades

- Current system magnetic field noise: 1.7 fT $Hz^{-1/2}$
- Realistically achievable upgrade: 0.4 fT $Hz^{-1/2}$
- Signal-to-noise ratio improvement of a factor of 4 enables one of the following:
    - Improve in-plane spatial resolution by a factor of 2 in each direction
    - Improve T_1-contast-to-noise ratio by a factor of 4
- More clinically useful system: multichannel for greater coverage?
- Biggest challenge: 300mT polarizing field over a useful volume

Future Directions for Low-Field MRI

- Combine low-field MRI with existing technology for magnetoencephalography (MEG)
- Low-cost "open" MRI system
  - Imaging hand, elbow, foot, knee…..
  - Imaging tumors--especially breast and prostate--with T_1-weighted contrast
  - MRI-guided biopsy
  - Imaging cryosurgery
  - Measuring tissue temperature during rf heating
  - Monitoring T_1 in bone marrow to monitor effects of chemotherapy or radiation therapy